

## **High Heat Flux Cooling Technologies Using Microchannel Evaporators: Fundamentals and Challenges**

CHENG, Lixin and XIA, Guodong

Available from Sheffield Hallam University Research Archive (SHURA) at:

<https://shura.shu.ac.uk/31091/>

---

This document is the Accepted Version [AM]

**Citation:**

CHENG, Lixin and XIA, Guodong (2022). High Heat Flux Cooling Technologies Using Microchannel Evaporators: Fundamentals and Challenges. Heat Transfer Engineering. [Article]

---

**Copyright and re-use policy**

See <http://shura.shu.ac.uk/information.html>

# High Heat Flux Cooling Technologies Using Microchannel Evaporators: Fundamentals and Challenges

Lixin Cheng<sup>a,b</sup> and Guodong Xia<sup>a,\*</sup>

*<sup>a</sup>Beijing Key Laboratory of Heat Transfer and Energy Conversion, Beijing University of Technology,*

*Beijing 100124, P. R. China*

*<sup>b</sup>Department of Engineering and Mathematics, Sheffield Hallam University, City Campus, Howard Street,*

*Sheffield S1 1WB, UK*

## **Abstract**

Flow boiling in multi micro-channel evaporators is a promising approach to cooling high heat flux in many devices. Understanding of the fundamentals of flow boiling in multi microchannel evaporators is urgently needed. This paper presents a critical review on the research of flow boiling phenomena in microchannels. First, classifications of macro- and micro-channels are briefed. Then, studies on flow boiling in multi microchannels with plain surface are analyzed. Next, studies of flow boiling in multi microchannels with various enhanced technologies are analyzed. Finally, heat transfer mechanisms and development of prediction methods are discussed. According to the critical review and analysis of the current research on the fundamental issues and challenges of flow boiling in micro-channels, future research needs have been identified and recommended. In general, systematic and accurate experimental data of flow boiling in micro-channels are needed by using advanced measurement technologies. In particular, optimal design of microchannel evaporators with plain surface and enhanced structures is lacking and should be investigated. The physical mechanisms of flow boiling should be further investigated based on the

corresponding flow patterns. Furthermore, mechanistic prediction methods should be developed. Furthermore, systematic experimental, analytical and modelling studies on transient flow boiling phenomena in micro-channels should be conducted to understand the physical mechanisms and develop the theoretical models.

\*Address correspondence to Prof. Guodong Xia, Beijing Key Laboratory of Heat Transfer and Energy Conversion, Beijing University of Technology, Beijing 100124, P. R. China. E-mail: [xgd@bjut.edu.cn](mailto:xgd@bjut.edu.cn).

## Introduction

Advanced reliable and effective high heat flux cooling technologies are crucial in a wide spectrum of industrial processes such as high power electronics, microelectronics, micro-processors in the computer and information technology, micro reactors, microfluidics, fuel cells, turbine blades, concentrator photovoltaic systems, battery packs in hybrid vehicles, advanced military avionics, defense radars, directed-energy lasers, electromagnetic weapons, space, thermal power plant and nuclear energy etc. [1-6]. Breakthroughs in many of today's cutting-edge technologies require advanced high heat flux and ultra high heat flux cooling technologies which are becoming increasingly dependent upon the ability to safely dissipate enormous amounts of heat from very small areas [7-16,7-9]. Two ranges of heat flux can be loosely identified relative to the magnitude of the heat dissipation and the type of coolant permissible in a particular application. These are the high fluxes of  $10^2 - 10^3$  W/cm<sup>2</sup>, and the ultra high fluxes of  $10^2 - 10^5$  W/cm<sup>2</sup> [2]. The higher heat fluxes must be removed while maintaining the material temperatures below prescribed limits, for example, the current high heat flux for power electronics in electric vehicles reaches up to 300 W/cm<sup>2</sup> at the chip level, while in some applications, such as defense power electronics, it can reach up to 1000 W/cm<sup>2</sup> [2, 6, 10-16]. Over the past decades, the cooling schemes such as pool boiling, detachable heat sinks, channel flow boiling, microchannel and mini-channel heat sinks, jet-impingement and sprays are discussed and compared relative to heat dissipation potential, reliability, and packaging concerns [2, 4 6, 9-14]. Of the available high heat flux cooling technologies, flow boiling in multi micro-channel evaporators is one of the most promising cooling solutions for cooling the high power density devices due to (1) the high heat transfer during boiling, (2) the large heat transfer area per unit fluid flow volume, (3) compact heat sink size, (4) small flow rate of coolant and (5) low pumping power. However, fundamentals and technology innovations of

flow boiling in micro-channel evaporators such as heat transfer performance heat transfer mechanisms, CHF, flow regimes, two phase instabilities, pressure drop, two phase flow instabilities, transient heat transfer behaviors and heat transfer enhancement technologies are urgently needed in order to understand the flow boiling phenomena and physical mechanisms, develop prediction methods and optimize and design suitable micro-channel evaporators with plain and enhanced structures for cooling high heat flux and ultra high heat flux devices in various technological applications [1, 2, 6, 9-11].

Over the past decades, efforts have been made to understand the fundamentals of flow boiling heat transfer performance, flow regimes, CHF, pressure drop and two-phase flow instabilities of conventional parallel microchannels with plain surface. In particular, stability of liquid vapor two-phase flow and is the key to the efficiency and safety of heat dissipation of high heat flux devices [1, 6, 15]. Flow instabilities may greatly affect flow boiling heat transfer and CHF in microchannel evaporators. Due to the reduced influence of gravity, surface tension and other interfacial forces become prominent for flow boiling in microchannels, the flow boiling heat transfer and two phase flow characteristics in microchannel evaporators are quite different from those in macro-channel evaporators. However, they are less understood than those in macro-channels. In particular, advanced measurement techniques specially for microscale flow boiling phenomena and characteristics such local flow boiling heat transfer characteristics, CHF, flow patterns, pressure drop and flow instabilities are urgently needed. Although numerous studies have been conducted over the past decades, quite different results and mechanisms have been obtained from one research to another. There are big challenges in this research field.

Enhancement of flow boiling heat transfer and CHF and stability of vapor liquid two phase flow in micro-channel evaporators are important to meet the high heat flux cooling requirements [17-20]. Over the past years, extensive studies have been conducted to enhance flow boiling

performances in microchannels in terms of heat transfer coefficient, CHF and stabilization of two-phase flows. Various heat transfer enhancement approaches including modifying surface properties, intensifying mixing or disturbance and enhancing nucleate boiling have been exploited to significantly increase flow boiling heat transfer performances and CHF in multi-microchannel evaporators [17, 18]. Furthermore, enhanced microchannels with various surface structures have also attracted much attention to mitigate two-phase flow instabilities in flow boiling. Artificial micro cavities, porous layers and nano coatings have been proposed to promote bubble nucleation, increase heat transfer areas, and mitigate rapid bubble growth in stabilities. Using nanofluids is another approach to enhance boiling heat transfer [13, 19-22]. However, the fouling, clogging, sedimentation and erosion may do harm to the cooling devices and therefore, nanofluids are not suitable for flow boiling in microchannel evaporators [13, 22].

Advanced measurement technologies are the key to obtaining accurate experimental results in the research of flow boiling in microchannel evaporators. Precisely measuring local flow boiling heat transfer in microchannels is difficult for commonly-used thermal sensors. Verification of heat transfer mechanisms based on direct observation of fundamental heat transfer phenomena at a small spatiotemporal scale is insufficient. The available research results of flow boiling in microchannels are quite different and contradictory at similar experimental conditions [1, 9, 14, 23, 24]. Some studies show too much high measured heat transfer coefficients and CHF data but did not explain the physical mechanisms for such high values. The results might not be correct due to using the macroscale measurement sensors for microscale flow boiling and thus resulted in big errors or even wrong results [11]. The prediction methods based on the experimental data with big errors or incorrect data are not able to predict flow boiling heat transfer coefficient and CHF in microchannel evaporators. Therefore, adopting advanced measurement technologies specially developed for microscale is crucial in the research of flow boiling phenomena in microchannel evaporators.

Furthermore, careful calibration of the measurement sensors and verification of thermal balance should be done for the experimental rig are essential when conducting the research. Proper data reduction methods should be adopted [1].

Water is an excellent working fluid with high latent heat and often used for flow boiling in experimental studies. However, the stringent material and electrical compatibility requirements in many applications prohibit the use of water in direct contact with current-carrying components, hence the need to use low boiling point dielectric fluorochemical coolants for cooling high power devices. For example, FC-72 has a saturation temperature of 56.6°C at atmospheric pressure and HFE-7100 has a saturation temperature of 61°C at atmospheric pressure, respectively. These temperatures are low enough to maintain moderate device temperatures but high enough to permit discharge of the heat to an ambient air an ambient air stream. The thermophysical properties essentially affect the cooling efficiency for traditional heat transfer coolants. Environmental issues and the useful physicochemical properties have made the fluorinated liquids (“Fluorinert” and “Novec” engineered fluids, i.e., the FC series and HFE series) excellent alternatives that have received much attention, especially the recently developed HFE series with superior environmental properties. However, dielectric fluorinated liquids still have some key drawbacks as phase change working fluids, such as poor thermophysical properties such as latent heat and low surface tensions compared with water. Using flow boiling for high heat flux cooling is adopted by taking the advantage of high latent heat. In this aspect, water has much higher latent heat than other fluids. Therefore, many attempts have been undertaken to improve the microchannel flow boiling heat transfer characteristics of dielectric fluorinated liquids, mainly relying on heat transfer enhancement approaches such as using artificial micro cavities, porous layers and nano coatings etc. to promote bubble nucleation and increase heat transfer areas in microchannel evaporators.

Flow boiling in multi micro-channel evaporators is one of the most promising approaches to cooling high heat flux in high power devices. However, there are challenges of applying this approach because advanced knowledge of heat transfer performance, transient heat transfer, critical heat flux (CHF), two phase flow instabilities, pressure drop physical mechanisms, heat transfer enhancement and optimal design of the microchannels with various structures have not yet fully established. The objective of this paper is to conduct a critical review on the existing studies regarding microchannel flow boiling by analyzing the flow boiling data, phenomena and mechanisms accounting for the effects of channels size, bubble dynamics and flow regimes in both conventional microchannel evaporators with plain surfaces and enhanced microchannel evaporators with various structures. The challenges and future research requirements for fundamental and advanced knowledge of flow boiling, mechanisms, development of prediction methods and optimal design of microchannel evaporators have been identified and recommended according to the analysis and discussion in this review.

### **Classifications of macro- and micro-channels**

Various definitions of microchannels based on the engineering applications, bubble confinements and dimensionless numbers have been proposed and summarized in [1, 8, 9, 12, 23-25]. However, the transition between micro- and macro- channels has neither been well defined nor seriously experimentally investigated [11]. The confinement number has been given different values according to individual observations and experimental data with limited test fluids, test channels and test conditions by various researchers. Although a number of such criteria are available, no universal agreement has been reached according to the dimensionless numbers so far [1, 25].

Kew and Cornwell [26] proposed the Confinement number  $Co$  for the distinction of macro- and micro-channels as follows:

$$Co = \frac{1}{D_h} \sqrt{\frac{\sigma}{g(\rho_l - \rho_g)}} \quad (1)$$

when the confinement number  $Co$  is less than 0.5, the channel is considered as microscale channel.

Mehendale et al. [27] defined various small and mini heat exchangers in terms of hydraulic diameter  $D_h$ , as follows:

- Micro heat exchanger:  $D_h = 1 - 100 \mu\text{m}$ .
- Meso heat exchanger:  $D_h = 100 \mu\text{m} - 1 \text{ mm}$ .
- Compact heat exchanger:  $D_h = 1 - 6 \text{ mm}$ .
- Conventional heat exchanger:  $D_h > 6 \text{ mm}$ .

Based on engineering practice and application areas such as refrigeration industry in the small tonnage units, compact evaporators employed in automotive, aerospace, air separation and cryogenic industries, cooling elements in the field of microelectronics and micro-electro-mechanical-systems (MEMS), Kandlikar [8] defined the following ranges of hydraulic diameters  $D_h$  which are attributed to different channels:

- Conventional channels:  $D_h > 3 \text{ mm}$ .
- Minichannels:  $D_h = 200 \mu\text{m} - 3 \text{ mm}$ .

It should be realized that the transition from macro-channels to micro-channels is a continuous process and should correspond to the flow regime, heat transfer behaviors, CHF and the physical mechanisms. Furthermore, relating flow regime behaviors to the corresponding flow boiling heat transfer and gas liquid two phase flow behaviors is a practical and effective method to develop mechanistic prediction models or methods for classifying macro- and micro-channels [28-32]. This has been validated by the flow pattern based  $\text{CO}_2$  flow boiling model of Cheng et al. [28-

30], which covers both macro- and micro-channels for CO<sub>2</sub> flow boiling heat transfer and two phase flow. Their generalized flow pattern based CO<sub>2</sub> flow boiling heat transfer model predicts both macro- and micro- channel flow patterns and heat transfer reasonably well [14, 33-35]. Therefore, the macro- and micro- channels may be classified according to the flow boiling heat transfer characteristics, mechanisms and the corresponding flow regimes. A mechanistic distinction criterion for macro- and micro-channels may be of practice and effectiveness in developing new flow boiling heat transfer prediction models. Such a criterion is not yet available and should be developed in future.

### **Critical review of the studies on flow boiling in multi-microchannel evaporators with plain surface**

Flow boiling in multi-microchannel evaporator is one of the most promising heat transfer technologies for high heat flux cooling by utilizing the latent heat of evaporation of a working fluid to remove the heat generated in high power devices [1-5]. As a result of the better thermal performance compared to other cooling processes, better axial temperature uniformity, hot spots cooling capability for cooling electronic chips and elements, reduced coolant flow rates and smaller pumping powers can be obtained in micro-channel evaporators. Over the past decades, extensive studies of flow boiling in micro-channel evaporators have been conducted to understand the phenomena, mechanisms and design of heat sink for high heat flux cooling [36-50]. Several comprehensive reviews have been presented to address the fundamentals and applications of flow boiling in microchannels by Cheng and Xia [1], Karayiannis and Mahmoud [6], Kandlikar [8], Cheng [9], Prajapati and Bhandari [47], Ribatski et al [48] and Tibirica and G. Ribatski [49].

In general, flow boiling occurs in multi micro-channels made in silicon or copper cooling elements attached to CPUs or high power density devices, or directly in the silicon chip itself.

Figure 1 shows the silicon die used as the test section by Agostini et al. [51]. It is 1 mm thick and 31×31 mm<sup>2</sup> in size. Multi microchannels have been etched into the upper face with an inductively coupled plasma etching process (dry etching) and are shown highly magnified in Fig. 2 (the magnification is increased in the successive three pictures starting from the top. The second and third pictures represent a close-up on one wall of the rectangular micro-channels). There are 67 parallel channels, which are 20 mm long, 223 μm wide and 680 μm high with a fin width of 80 μm. The schematic diagram is shown in Fig. 3 (a). Cheng and Thome [35] have presented simulation results of flow boiling and two phase frictional pressure drop of CO<sub>2</sub> in the same multi-microchannel evaporator as the one by Agostini et al. [51]. Figure 3 (a) shows schematic of the multi micro-channel evaporator for chips cooling with the CO<sub>2</sub> flow boiling. Figure 3(b) shows the comparison of the simulated base temperatures using CO<sub>2</sub> as the working fluid with the Cheng et al. flow patterns based mechanistic heat transfer models [29, 30] and the measured basR236fa flow boiling in the multi microchannel evaporator shown in Fig. 3(a). It has been found that the superior heat transfer performance can be achieved with flow boiling in the micro-channel evaporator.

Flow boiling characteristics and mechanisms such as heat transfer, CHF and two phase pressure drops in micro-channels are quite different from those in conventional channels according to the available studies [3-8]. Due to the confined space effect, two phase flow phenomena such as flow regimes, backflow and flow instabilities need to be understood for various working fluids and operation conditions [1, 6, 47]. There are challenges in achieving comprehensive knowledge and technology development of flow boiling in multi microchannel evaporators, therefore, analysis of the flow boiling heat transfer, CHF, mechanisms, flow regimes and flow instabilities in multi microchannel evaporators with plain surface are critically reviewed and analyzed in this section.

### ***Flow boiling heat transfer, flow regimes, mechanisms and CHF in microchannel evaporators***

Over the past decades, a large number of experimental studies of flow boiling in multi-microchannel evaporators have been extensively conducted to understand the fundamentals of flow boiling phenomena and practical design for cooling systems of micro-channel heat sinks. Multi microchannels with various shapes such as rectangular, trapezoidal, circular and triangular etc. were used in the experiments. Various fluids such as water, refrigerants, dielectric fluids and others have been employed as the working fluid in the experiments under different test conditions. The channel size and confinement have a significant on the flow boiling characteristics, flow regimes, two phase flow instabilities, CHF and physical mechanisms. Compared to those in macro-channels, flow boiling phenomena in micro-channels have not yet been well understood. The available studies of flow boiling heat transfer phenomena in micro-channels have exhibited contradictory results although a large amount of experimental work, theory and prediction methods for flow boiling in microchannels have extensively been conducted so far [4]. The recent studies on the fundamentals of flow boiling in multi microchannel evaporators are focused on here. Table 1 summarizes the selected experimental studies on flow boiling heat transfer, flow regimes, CHF, mechanisms, two phase pressure drop and two phase instabilities in micro-channels.

Agostini et al. [51-53] et al. measured local heat transfer coefficients and CHF for refrigerant R236fa and R245fa flow boiling in a silicon multi-microchannel heat sink for a large range of heat fluxes, mass velocities and vapor qualities. The heat sink is shown in Fig. 1 and Fig. 3 (a). Figure 4 shows their measured local heat transfer coefficient of R236fa versus the local vapor quality at mass velocities from 281 to 1501 kg/m<sup>2</sup>s and fixed heat fluxes of 37.7 and 103.3 W/cm<sup>2</sup>. From their study, three main heat transfer trends were outlined. At the low heat fluxes, vapor qualities and mass velocities, the heat transfer coefficient increases with increasing the vapor quality and is independent of the heat flux and mass velocity. At medium heat fluxes, the heat

transfer coefficient is almost independent of the vapor quality and increases with increasing the heat flux and slightly dependent on the mass velocity. At very high heat fluxes, the heat transfer coefficient increases slightly with increasing the mass velocity and decreases with increasing the heat flux. This later trend is probably due to intermittent dry-out before reaching CHF [52]. These results contrast significantly with macroscale flow boiling trends. In particular, the convective boiling regime does not seem to exist in the microchannels. The predominance of heat transfer coefficients mainly dependent on heat flux reported by a number of studies is confirmed. It should be pointed out that quite different experimental heat transfer results, trends and mechanisms of flow boiling in microchannels have been obtained by various researchers in the literature [1, 48, 49]. Even for the results by Agostini et al., quite different heat transfer trends have been obtained. Figure 5 shows a logic diagram of the major heat transfer trends identified for R245fa and R236fa in their study. It can be seen that the trends are very similar for both fluids with two exceptions. For R245fa the heat transfer coefficient is more dependent on the mass velocity than for R236fa. At high mass velocities and low heat fluxes, the heat transfer coefficient of R245fa shows a fourth peculiar trend (iv): the U shape with vapor quality and a decrease in heat transfer coefficient with increasing heat flux. However, this combination of operational parameters corresponds to very low wall-fluid temperature differences (typically around 1 K) and very low vapor quality (less than 5%) where the experimental uncertainty is the highest ( $\pm 30\%$ ). Furthermore, heat transfer coefficients measured for low heat flux  $q$ , low vapor quality  $x$  and high mass velocity  $G$  are likely to be influenced by the bubbles generated by the inlet orifice by cavitation. Similar to other studies, different combination of operational parameters in flow boiling may result in quite different heat transfer trends which represent different heat transfer mechanisms. Different microchannels with various shapes and dimensions may also affect the heat transfer trends and mechanisms. Different fluids have quite different thermal physical properties which have a significant effect on the heat

transfer behaviors and mechanisms. It must be pointed out that quite big discrepancy among the available studies regarding the heat transfer coefficients, trends and mechanisms even for the same fluids at similar conditions but it is difficult to explain such results [11].

CHF refers to the value of heat flux at which the local heat transfer coefficient decreases sharply due to the replacement of liquid by vapor adjacent to the heat transfer surface. In most cases, once this limiting condition is detected as a sharp rise of surface temperature, the heating power must be cut before the component physically burns out. For designing the cooling systems for micro-processor chip and high power devices, advanced knowledge of the CHF is essential in determining the upper operating limit of the cooling systems for safe operation. Cheng [9] has presented a comprehensive review of the studies on CHF phenomena during flow boiling in micro-channels and nucleate pool boiling in confined spaces [9]. There are challenges of studies on CHF in microchannels. Although a large number of studies on CHF in multi microchannel evaporators have been conducted over the past decades, quite different results have been obtained from one study to another. Furthermore, the prediction methods are mostly based on limited working fluids and experimental conditions but often be extended to other fluids and conditions, thus give poor prediction results in most cases. Apparently, generalized prediction methods are not yet available for micro-channel evaporators so far as of the lack of accurate CHF data and mechanisms.

In recent years, research on CHF in microchannel evaporators continues increasing to understand the fundamentals [53-55]. Park and Thome [54] conducted experimental study of CHF at low mass velocities and low pressures for two microchannel heat sinks. One has 20 parallel rectangular channels with 467  $\mu\text{m}$  wide and 4052  $\mu\text{m}$  deep and the other one has 29 rectangular channels with 199  $\mu\text{m}$  wide and 756  $\mu\text{m}$  deep. Figure 6 shows the experimental base CHF versus mass velocity in the microchannel evaporator with the channel depth  $H = 4052 \mu\text{m}$ . R134a was tested at the saturation temperature of 25°C with different subcooling degrees and the mass velocity

in the range of 100 – 400 kg/m<sup>2</sup>s. While CHF increases with increasing the mass velocity, its rate of rise becomes less at higher mass velocities. On the other hand, CHF increases moderately with increasing the inlet subcooling. Consequently, the highest base heat flux reaches 342W/cm<sup>2</sup> at the mass flux of 400 kg/m<sup>2</sup>s and the subcooling of 20 K. This is the highest value reached in their study. This value however should not be taken as the maximum for the test conditions, as the test geometry is in no way optimized to find this limit. Figure 7 shows the experimental base CHF versus mass velocity in the microchannel evaporator with the channel depth  $H = 756 \mu\text{m}$  at the same test conditions as in Fig. 6. As the mass velocity increases, CHF also increases and shows the same trend as that in Fig. 6. However, no significant subcooling effect was observed in their study. This means the channel depth corresponding the aspect ratio may have a significant effect on CHF but systematic knowledge of the effect of aspect ratio on CHF for different experimental conditions and working fluids should be further conducted.

It should be pointed out here that for both flow boiling heat transfer, CHF and mechanisms in microchannel evaporators, one key point is to adopt advanced measurement technologies specially for microscale flow boiling experiments. Properly designed experimental systems are needed and careful calibrations of the sensors and the whole experimental systems should be performed. Proper data reduction methods should be used. Deep analysis of the results and physical mechanisms are extremely important but are often missing in many published papers [1, 9]. Aspect ratio has a significant effect on the flow boiling heat transfer, flow regimes and CHF [62, 64]. However, systematic knowledge of the effect of aspect ratio on flow boiling microchannel evaporators is needed. Effort should be made to develop generalized mechanistic prediction methods for flow boiling heat transfer and CHF in future while systematic and accurate experiments should be conducted to obtain proper test data at first.

Understanding flow boiling heat transfer, CHF and mechanisms should be related to the corresponding flow regimes in micro-channel evaporators [1,23-25,29-32]. Lee and Mudawar [50] investigated the two-phase heat transfer characteristics of two large micro-channel evaporators in the vapor compression loop using R134a as refrigerant for the development of a thermal management system operating in vapor compression mode to tackle high heat sink temperatures in future manned space endeavors. Both evaporators feature parallel micro-channels with identical  $1 \times 1\text{-mm}^2$  cross-section. The evaporators are connected in series, with the smaller 152.4-mm long evaporator situated upstream of the larger 609.6-mm long evaporator. They conducted systematic assessment of the dominant heat transfer mechanisms using both heat transfer measurements and high-speed video. Figure 8(a) shows the variation of the two-phase heat transfer coefficient along the avionics heat exchanger (H/X) for  $q = 44,401.1 \text{ W/m}^2$  and  $G = 340.23 \text{ kg/m}^2\text{s}$  and figure 8(b) shows the dominant heat transfer mechanisms along the micro-channel for low, mid, and high vapor quality conditions. The dominant flow patterns and corresponding heat transfer mechanisms can be summarized here as (i) For the avionics H/X, which is associated with both low and high vapor qualities, both flow patterns and heat transfer mechanisms change drastically for different vapor quality ranges; (ii) For low vapor qualities of  $x_e < 0.36$ , bubbly and mostly slug flow are dominant, and heat transfer is associated mostly with nucleate boiling; (iii) For mid vapor quality range of  $0.36 < x_e < 0.50$ , annular flow is prevalent and heat transfer is the result of convective boiling across the annular film; (iv) At  $x_e = 0.5$ , incipient dryout marks the point where the heat transfer coefficient begins to decrease appreciably with increasing the vapor quality because of localized dryout of the annular film. (v) While annular flow persists in the high range of  $0.50 < x_e < 0.74$ , increasing the vapor quality increases the size and number of dryout regions; (vi) Complete dryout is encountered around  $x_e = 0.74$ , following which mist flow prevails, where the wall is mildly cooled by liquid droplets deposited from the vapor core. Overall, it is shown low qualities

are associated with slug flow and dominated by nucleate boiling, and high qualities with annular flow and convective boiling. Important transition points between the different heat transfer regimes are identified as (1) intermittent dryout, resulting from vapor blanket formation in liquid slugs and/or partial dryout in the liquid film surrounding elongated bubbles, (2) incipient dryout, resulting from dry patch formation in the annular film, and (3) complete dryout, following which the wall has to rely entirely on the mild cooling provided by droplets deposited from the vapor core. They have well documented the flow boiling mechanisms according to the measured heat transfer data and the corresponding flow patterns in their study.

However, quite anomaly flow boiling heat transfer and CHF trends in microchannel evaporators are presented in some publications but they cannot be explained according to the corresponding flow boiling mechanisms or no corresponding flow patterns were observed in some studies [1, 9, 48]. As pointed out by Cheng and Xia [1], big discrepancies among the experimental data from different independent laboratories may be caused due to different surface roughness of the test channels, channel dimension uncertainties, improper data reduction methods, flow boiling instabilities, improper designed test facility, test sections and experimental procedures. In some cases, the published results are unreasonable such as too big or too small heat transfer coefficients, some or complete wrong heat transfer behaviors and trends and correlations of various parameters and physical properties even if they have been published. Furthermore, some flow boiling heat transfer correlations and models were proposed by simply regressing limited experimental data at limited test parameter ranges without considering the heat transfer mechanisms. Therefore, it is necessary to evaluate these correlations to validate their applicability before using these correlations. In fact, in most cases, such correlations do not work properly for other working fluids and operation conditions, Cheng and Xia [1] analyzed and evaluated a large amount of experimental data and a number of the correlations and obtained such conclusions.

Due to the large discrepancies between experiment results from different researchers, systematic knowledge of understanding the fundamentals of flow boiling including characterization, mechanisms and model development in micro-channels is still urgently needed. Furthermore, a number of heat transfer prediction methods such as correlations and models have been proposed for flow boiling heat transfer in microscale channels. However, nearly all these methods were based on limited test fluids, channel shapes and diameters under limited parametric conditions such as limited range of saturation temperatures, mass fluxes, heat fluxes and working fluids etc. Therefore, the extrapolation of the available prediction methods to other fluids and channels do not work properly [41]. Further effort should be made to develop unified mechanistic prediction methods for flow boiling based on the physical mechanisms and flow patterns.

### ***Flow boiling instabilities in multi microchannel evaporators***

Flow instabilities can result in thermal limits being exceeded, forced mechanical vibrations, fatigue and failure of system components, poor system control, and difficult normal operations and system safety. In particular, sustained flow oscillations may cause the local heat transfer characteristics to deteriorate and induce CHF. Flow boiling instabilities are more sensitive in micro/confined flow passages. Due to the confined space, an elemental disorder during flow boiling triggers the unstable two phase flow and heat transfer conditions that ultimately lead to instabilities. Over the past years, many studies have been conducted to understand the flow boiling instabilities in microchannels as listed in table 1. Figure 9 shows the major causes for the flow boiling instabilities in microchannel evaporators. Peculiar bubble dynamics and flow regimes may explain the phenomena and mechanisms of instabilities in flow boiling [47]. First, vapor bubbles originate during flow boiling, then the bubble clogging follows due to rapid bubble growth/elongation which results in flow reversal as shown in Figs. 9. This peculiar bubble dynamics is caused by inherent

confined geometry of the microchannels, operating and flow conditions, thermal physical properties and vapor quality of working fluid along with microchannels. Large inlet subcooling condition further accelerates the two-phase instabilities in microchannels. Parallel channel interactions and inlet compressibility are well identified factors to elevate and accelerate the adverse bubble dynamics. Severe instabilities start with bubble clogging followed by rapid bubble growth and reverse flow of the vapor in the inlet section. In addition to these, parallel channel interactions, upstream compressibility trigger the instabilities. All these three factors independently or cumulatively cause the instabilities in the microchannels,

Furthermore, periodic flow oscillations are commonly encountered in two-phase micro-channels because bubbles grow rapidly to occupy the entire cross-section. These instabilities are manifest in periodic oscillations in mass velocity, which are responsible for pressure oscillations between the inlet and outlet plenums. Lee et al. [57] investigated the interfacial behavior and heat transfer mechanisms associated with flow boiling of R-134a in a micro-channel evaporator. The test evaporator consists of 100 of  $1 \times 1 \text{ mm}^2$  square micro-channels. Large length of the micro-channels used (609.6 mm) is especially important to capturing broad axial variations of both flow and heat transfer behavior. The fluid was supplied to the test evaporator in subcooled state to enable assessment of both the subcooled boiling and saturated boiling regions. They employed a combination of temperature measurements along the microchannels and high-speed video to explore crucial details of the flow, including dominant flow regimes, flow instabilities, and downstream dryout effects. Figure 10 shows a series of schematics of transient flow patterns observed in their experimental study based on extensive analysis of video records. From a temporal standpoint, a single oscillation period consists of six sub-periods. Notice that the micro-channel is divided spatially into four distinct sections; flow within each varies during the successive sub-periods [57]. Unlike macro-channel flow boiling where flow regimes can be clearly demarcated,

flow regimes in the micro-channels are associated with transient fluctuations that are induced by flow instabilities. The dominant flow behavior and associated dryout effects are characterized with the aid of a new transient flow regime map and a dryout map, respectively. Two sub-regions of the subcooled boiling region, partially developed boiling and fully developed boiling, are examined relative to dominant interfacial and heat transfer mechanisms in their study. The saturated boiling region is shown to consist of three separate sub-regions: nucleate boiling dominated for the vapor qualities below 0.3, combined nucleate and convective boiling for the vapor qualities between 0.3 and 0.5, and convective boiling dominated for the vapor qualities above 0.5. For the vapor qualities larger than 0.5, dryout begins to take effect, causing a gradual decrease in the heat transfer coefficient followed downstream by a more severe decrease. Their observed mechanisms are quite different from those by Agostini et al. [52] described in the forgoing. The effect could be due to the effects of instabilities, flow regime, unstable flow and heat transfer, different microchannels, working fluids and test conditions.

One key point is to eliminate or damp the instabilities in microchannels. Various methods have been conducted, such as restricted. Modified surface properties or control of operation conditions [47]. In general, microchannels with inlet restrictors (IRs) can suppress the reversal two-phase flows. Furthermore, with the enhanced two-phase flow stability, flow boiling heat transfer and CHF can be noticeably improved. Hedau et al. [65] experimentally investigated the combined effect of nanostructure and inlet restrictor on reducing the instabilities during flow boiling in parallel microchannel heat sinks. Four types of microchannel heat sinks were used in their study: plain microchannels, microchannels with inlet restrictor, nanostructured microchannels and nanostructured microchannels with inlet restrictor. Different flow regimes such as bubbly flow, slug flow, annular flow and partial dryout have been observed at various heat fluxes and mass flow velocities. The fluctuations of pressure, temperature, and mass flow velocity are characterized in

each flow regime. It is found that the fluctuations increase with increasing power input, which is primarily due to backflow of vapor in the upstream direction of flow. The microchannel with inlet restrictor is more effective in reducing fluctuations and result in less surface temperature compared to the baseline case of plain microchannel without restrictor at the same test conditions. Moreover, for the nanostructured surface microchannel with the inlet restrictor, the effectiveness in reducing fluctuations increases at higher heat flux and also produces less surface temperature compared to other types of microchannels. Figure 11 (a) and (b) displays the transient variation of fluctuations of pressure drop at various temperatures and mass flow rates for the heat fluxes of 81 and 137 W/cm<sup>2</sup> respectively at the mass velocity of 250 kg/m<sup>2</sup>s. It is observed that the pressure drop fluctuations in nanostructured microchannels without the inlet restrictor ( $P_{ch,nano}$ ) are less than that in the plain microchannels ( $P_{ch}$ ). However, when both the modifications, inlet restrictor and nanostructured surface are incorporated in the  $P_{ch}$ , it is found that the peak to peak pressure differences is further reduced. In nanostructured microchannels, the capillarity due to superhydrophilic nanostructures allows quick rewetting of microchannel wall in the annular flow regime. This mechanism reduces the two phase frictional resistance in the microchannels. Thus, a further reduction of pressure drop fluctuations is observed in  $IR_{ch,nano}$ . The similar characteristics of pressure drop fluctuations are also observed in Fig. 11(c) and (d) for higher mass velocity of 500 kg/m<sup>2</sup>s. The  $IR_{ch,nano}$  produces more fluctuations as compared to the  $IR_{ch}$  due to the presence of more active nucleation sites. The rate of vapor generation is more in the nanostructured channels due to which the tendency of vapor backflow is more in the  $IR_{ch,nano}$ . Figure 12(a) and (b) illustrates the fluctuations of the transient surface temperatures at the heat fluxes of 81 and 137 W/cm<sup>2</sup> and the mass velocity of 250 kg/m<sup>2</sup>s. The peak to peak temperature differences decrease when the  $P_{ch}$  is modified with the inlet restrictor or the nanostructured surface. However, when the  $P_{ch}$  is designed using both the inlet restrictor and the nanostructured surface, the peak to peak temperature

difference is further decreased. The surface temperature is minimum in the  $IR_{ch, nano}$  compared to all other considered microchannels. The combined effects of inlet restrictor and nanostructured surface enhance the active nucleation-site density and also increase vapor entrapment volume. The inlet restrictor increases fluid velocity, which increases the movement of vapor bubbles uniformly. Thus, the more stable and minimum surface temperature is observed in the  $IR_{ch, nano}$ . Hence, it can be concluded that the  $IR_{ch, nano}$  is more effective in reducing the surface temperatures with acceptable fluctuations of the surface temperature. Figure 12(c) and (d) show the transient fluctuations of the mass velocities in the  $P_{ch}$ ,  $P_{ch, nano}$ ,  $IR_{ch, nano}$  for the input mass flux of  $250 \text{ kg/m}^2\text{s}$  at the heat fluxes of  $81$  and  $137 \text{ W/cm}^2$ . The maximum fluctuations of  $485$ ,  $338$  and  $218 \text{ kg/m}^2\text{s}$  are observed for the  $P_{ch}$ ,  $P_{ch, nano}$ ,  $IR_{ch, nano}$ , respectively at the heat flux of  $81 \text{ W/cm}^2$ . As heat flux increases from  $81 \text{ W/cm}^2$ , the  $IR_{ch, nano}$  shows more fluctuations as compared to the  $IR_{ch}$ . At high heat fluxes, due to the presence of more active nucleation sites as compared to the plain channel, the vapor generation rate is more. This causes more fluctuations as compared to the  $IR_{ch}$ . The combination of inlet restrictor and nanostructured surface produces minimal fluctuations except at few heat fluxes, at which the active nucleation sites are more resulting in slightly increased fluctuations, but reduced surface temperature of the microchannel.

According to the foregoing analysis, it is important to relate the flow regimes and bubble dynamics to the heat transfer coefficient behaviors because they are intrinsically related to each other. In particular, for microchannel evaporators, well designed test facilities and accurate measurement systems are the key to obtaining accurate experimental flow boiling heat transfer and CHF data. The different heat transfer trends from various research groups may be explained by their respective heat transfer mechanisms and they may also due to many other affecting factors such as the measurement accuracy, channel size and shape, fluid types and the physical properties, the test parameter ranges, the data analysis and presentations etc. Different heating methods such as

fluid heating and electrical heating, measurement methods and different data reduction methods could result in quite big contradictory results. For instance, local and average heat transfer coefficients may be quite different, depending on how the wall and local saturation temperatures are determined. Furthermore, careful energy balance and validation of the measurement system should be done before performing the flow boiling experiments. In recent years, high-resolution temperature measurement techniques, such as MEMS sensors, high-speed infrared thermometry, and temperature sensitive paints have been developed, and they enable the direct measurement of the temperatures. The MEMS sensors are superior to other optical measurement techniques in terms of its spatiotemporal resolution and thus provide an accurate measurement method for local temperatures and heat fluxes. Therefore, advanced measurement techniques specially for microscale flow boiling should be used in the experiments.

It should be pointed out that the existing experimental results from the literature can hardly be compared against one or another since there is no accepted benchmark. Furthermore, the issue of the dominant heat transfer mechanisms is not well explored and explained according to the experimental data. In another word, researchers are in somewhat of a ‘dilemma’ to conclude which are the dominant flow boiling heat transfer and CHF mechanisms in their studies as sometimes their proposed heat transfer and CHF mechanisms actually do not describe their heat transfer coefficient trends properly. Therefore, careful and deep analysis of the experimental data and two phase flow phenomena in microchannel evaporators should be performed to provide valid heat transfer and CHF mechanisms for microscale flow boiling.

### **Enhancement of Flow boiling with structured microchannel evaporators**

Heat transfer enhancement techniques for nucleate boiling and flow boiling have been extensively invested for many years [66-71]. These methods may be applied to enhance flow

boiling heat transfer in microchannels as well [72, 73]. In recent years, a large number of studies have shown that flow boiling performances can be significantly enhanced by decorating microstructures, porous structure or surface modifications in microchannels, such as inlet/outlet restrictors, auxiliary channels and microcavities [74, 75].

Table 2 lists selected studies on enhancement of flow boiling heat transfer and CHF in microchannel evaporators. Many techniques have been explored to increase the nucleation site density such as microcavities, bridged or interconnected channels and nanowire coatings and others. Furthermore, enhanced methods have also been investigated to increase CHF to enlarge the working margin of high-power density electronics. Explosive boiling, two-phase instabilities and local dry-out are identified as three main factors that can trigger CHF. Various approaches have been developed to enhance CHF such as surface modifications to enhance rewetting, IRs to suppress flow instabilities, multiple micronozzles to enhance liquid supply. To prevent local dry-out, reentrant cavity and bridged or interconnected channels have been developed as effective methods to promote rewetting and hence, CHF. The micro-pin-fin array decorated on the bottom surface of the microchannels is effective in promoting the thin film evaporation and rewetting capability, leading to drastically enhanced heat transfer and CHF. Porous and grooved surfaces can be effective ways to generate thin liquid films.

Flow disruption structures enhance heat transfer by disrupting the normal development of thermal and flow boundary layers, reducing the thickness of thermal boundary layer, and preventing bubbles from blocking in two-phase boiling flow. A large number of flow disruption structures have been developed to enhance heat transfer in microchannel heat sinks. They can be roughly divided into two means, i.e., micro pin fins and cross-linked microchannels. Micro pin fins structures can interrupt and redevelop boundary layers, and increase flow mixing via vortices.

Therefore, heat transfer enhancement up to several times and a reduction of wall temperature rise can be obtained.

Pin fin structures can be also added to the microchannel side walls to promote boiling nucleation and break flow and heat transfer boundary layers. Xu et al. [78] proposed gradient-porous-wall microchannels with pin-fin arrays on the side walls as shown in Fig. 13(a). These structures could prevent fluid from exchanging along the flow direction and change confined bubble flow to un-confined bubble flow. Therefore, the porous-wall microchannel provided a new way to eliminate the two-phase flow instability of microchannel heat sinks. Following the above concept, Zong et al. [81] prepared gradient-porous-wall microchannel heat sink with the wall regions replaced by the gradient micro pin fin arrangement. Three regions, i.e., the densely/intermediate densely/sparsely pin fin region with the fin gap of 5  $\mu\text{m}$ /7.5  $\mu\text{m}$ /10  $\mu\text{m}$ , respectively, were formed to build the gradient-porous walls, as shown in Fig. 13(b). Flow boiling results showed that gradient-porous-wall microchannels induced a premature ONB and a very fast nucleate boiling flow in whole channel in less than 2 ms. The boiling flow instability was also suppressed, and the duration of two-phase flow was prolonged. Besides, Jia et al. [79] prepared rectangular porous-wall microchannels with uniform circular pin fins on the sidewall to provide numerous nucleation sites and introduce significant wicking effect to maintain the liquid rewetting as shown in Fig. 13(c). The porous-wall microchannels were found to reduce the wall superheat of ONB, enhance boiling heat transfer, and promote the CHF.

Cavity structures on the sidewall of microchannels can enhance flow boiling heat transfer. They can supply as ideal sites for bubble embryo growth. The increase in nucleation site density and the heat transfer enhancement can be thus expected. Several enhanced microchannels with various-shaped reentrant cavities on the sidewall have been developed as shown in Fig. 14. Kosar et al. [90] fabricated rectangular silicon microchannels with an array of 7.5  $\mu\text{m}$  wide interconnected

reentrant cavities on the sidewall as shown in Fig. 14(a). The flow boiling tests of water show that the convective boiling plays a leading role in high boiling number and Reynolds number, whereas nucleate boiling dominated in low boiling number and Reynolds number. Kuo et al. [91] developed microchannels with nonconnected reentrant cavities on the side wall as shown in Fig. 14(b), and investigated their flow boiling performance with the comparison of plain-wall microchannel without reentrant cavities. It shows that the microchannels with nonconnected reentrant cavities reduce the wall superheat of boiling incipience, alleviate the flow oscillation and improve the CHF to as high as  $643 \text{ W/cm}^2$  at the mass velocities of  $303 \text{ kg/m}^2\text{s}$  with deionized water as coolants. The microchannels with reentrant cavities promote bubbles nucleation and improve the reproducibility and uniformity of bubble generation. Furthermore, both microchannel with reentrant cavities and interconnected reentrant cavities can suppress the flow boiling instability of microchannels. Sitar and Golobic [92] studied flow boiling in rectangular microchannels with triangular, conical, round and a sharp edged reentrant cavities on the sidewall of the microchannels as shown in Fig. 14 (c). It shows flow boiling enhancement. Li et al. [93] integrated multiple micro-nozzles and reentrant microcavities on the sidewall of microchannels as shown in Fig. 14(d) to enhance flow boiling. These structures enhanced global liquid supply by four evenly distributed micronozzles, and mitigated local dry out by the capillary flow-induced sustainable thin liquid film resulting from an array of reentrant microcavities. They can achieve a CHF of  $1016 \text{ W/cm}^2$  with a 50% less mass velocity of  $680 \text{ kg/m}^2\text{s}$ , compared to the two-nozzle configuration.

High aspect ratio microchannels have the advantage of dissipating more heat per base area. However, flow boiling instability of bubble expansion towards upstream and downstream is more easily triggered once boiling starts due to the narrower channel width of high aspect ratio microchannel. Cheng and Wu [82] conducted experimental investigation of flow boiling heat transfer performance of deionized water in high-aspect-ratio (aspect ratio of 2.5) interconnected

microchannels with micro connection slots as shown in Fig. 15. Their results show that obviously earlier onset of nucleate boiling (ONB) in the interconnected microchannels is obtained as compared to that in plain-wall microchannels and almost no bubbly flow is observed in the interconnected microchannels. Significantly stable flow boiling from the incipience of boiling to near the CHF is obtained in the interconnected microchannels. It is observed that regular liquid film redevelopment and annular flow appear alternately among parallel microchannels. Figure 16 shows the variation of base heat flux with the wall temperature. Pronounced improvement of the heat flux dissipated at a fixed wall temperature can be achieved using the high-aspect-ratio microchannels. The reason is the base heat transfer area (direct contacting the heat source) is nearly 2.6 times the wall heat transfer area (contacting the fluid). This result demonstrates the superior advantage of the high aspect ratio microchannel for chip cooling.

Li et al. [86] investigated a novel capillary structure made from micro-pinfin fence fabricated in microchannels to rectify the usually chaotic and unstable two-phase flows during boiling processes. A highly stable and efficient single annular two-phase flow regime is demonstrated experimentally and visually on two distinguished fluids: DI-water with high surface tension and completely wetting fluid of HFE-7100. More importantly, sustainable thin film evaporation has been established and resulted in the formation of a highly desirable V-shaped heat transfer coefficient curve, i.e., achieving high heat transfer coefficients at high working heat fluxes. Figure 17 shows the development of conceptualization of their microchannels. In a traditional microchannel with smooth sidewall, as shown in 17(a), a very thin liquid film can be momentarily generated on the sidewalls and channel corners after vapor slugs expanding along the channel. To better illustrate the difference of thin liquid film profile, a microchannel was designed and fabricated with a smooth wall in one side (Fig. 17(a)), and a micro-pinfin fence in the other side (Fig. 17(b)). Fig. 1(c) shows a snapshot of liquid thin film development on both walls clearly

show the difference in terms of profile. On the smooth sidewall, the receding contact angle of liquid front is about  $5^\circ$  (in Fig. 17c), much smaller than the advancing contact angle about  $40 \pm 2^\circ$ . Under high heat fluxes, the thin liquid film would quickly evaporate, leading to a dry-out crisis, or premature CHF conditions. However, capillary microarchitectures (Fig. 17(b)) were designed and fabricated along each vertical wall inside microchannels can maintain thin liquid film. Once the liquid-vapor interface is established adjacent to micro-pinfin fence during the boiling process (Fig. 17(c)), a uniform thin liquid film, which serves as reconstructed two-phase boundary layer, was formed between the wall and micro-pinfin fence because of the induced capillary action. Figure 17(d) illustrates the profile of liquid film and occurrence of evaporation. The enhanced capillary action plays a key role in maintaining liquid film. Figure 18(a) shows typical V-shaped heat transfer coefficient curves, indicating a highly efficient boiling heat transfer process after establishing stable thin liquid film. In general, the heat transfer coefficients initially decrease with increasing the effective heat fluxes, and then they gradually increase after surpassing the turning point of the V-shaped curve. The V-shaped heat transfer coefficients curves are primarily related to the development of flow regimes. Figure 18(b) shows the effective heat transfer coefficient versus the exit vapor quality. At higher mass flow rates, the whole walls can be wetted and engaged in evaporation and boiling. However, at lower mass flow rates, sidewalls may not be fully wetted due to lack of sufficient working fluids.

According to the available studies, enhanced microchannels can be implemented via two directions. One is the alteration of microchannels walls or bottom surfaces, such as the preparation of reentrant micro-cavities, the addition of porous layer and nanostructures on the microchannel walls or bottom surface. These means are commonly able to enlarge heat transfer areas, increase bubble nucleation sites, change the surface wettability, and mitigate the severe two-phase instability or delay the early occurrence of CHF. The other one is to modify the flow passages, such

as flow disruption structures (e.g., micro pin fins or cross-linked microchannels), reentrant flow passages of microchannels, or porous based microchannels. These approaches generally contribute to enhance flow distribution and redevelopment thermal boundary layers, provide more passages for vapor flow, and modify the flow pattern. The promotion of bubble nucleation can be also obtained for porous microchannels. The above two directions of enhanced microchannels are able to promote the flow boiling enhancement in heat transfer coefficient, CHF or two-phase flow instability. However, there are no systematic design methods for the enhanced structures and techniques and no optimal design for the various structures. Systematic knowledge has not yet been established so far. Although various flow boiling mechanisms have been proposed to explain the flow boiling phenomena, they are mostly based on the existing mechanisms for nucleate pool boiling and flow boiling for conventional channels. Flow regimes are critical to understanding the microscale flow boiling mechanisms but microscopic observation of evolution of flow regimes is very limited in the current study. Furthermore, some studies have reported too much high heat transfer and CHF behaviors, which seem not to be true as there is limitation of the latent heat of the working fluids. This means that well designed experimental systems, advanced measurement technologies specially for micro-scale flow boiling, proper data reduction methods for various micro channels with enhanced structures and careful and deep analysis of the measured results and mechanisms are lacking.

## **Discussions**

According to the foregoing review, there are big challenges in the research of fundamentals of flow boiling in micro-evaporators although a large number of relevant studies have been conducted over the past decades. Several key aspects should be considered when conducting research in flow boiling in micro evaporators in future. First, selection of a proper working fluid should be carefully

considered. Water is utilized in a majority of research works due to its good thermophysical properties, cheapness and no environmental concerns. Its excellent boiling heat transfer performance is promising for high heat flux dissipations. Nevertheless, the feed water will keep rather much admixtures in spite of its careful and multilevel treatment. Refrigerants and dielectrics may be favorable in the electronic industry due to their low boiling points, whereas their heat transfer performances are not comparable to those of water. Therefore, it is necessary to select suitable working fluid for different applications. Second, various structured surfaces are used for enhancement of flow boiling heat transfer, CHF and stability of two phase flow. However, the fouling phenomena with contaminants for the porous coatings and nanostructures cannot be ignored for the selection of working fluid. Furthermore, under flow and fierce boiling conditions, the morphologies of nanostructures may change, which is prone to severe degradation, including deformation of nanotube, blockage of nanoscale pores or gradual detachment of nanostructure from heating surfaces. As a result, the performances of heat transfer coefficient and CHF may decrease in long-time operations. The durability of these enhanced surfaces has not been tested in the literature and should be considered in future research.

Flow boiling heat transfer in macro-channels is governed by two basic mechanisms of nucleate boiling dominant mechanism relating to the formation of vapor bubbles at the tube wall surface and convection dominant mechanism relating to conduction and convection through a thin liquid film with evaporation on the tube wall and at the liquid–vapor interface [94-97]. Flow boiling heat transfer and dryout mechanisms are intrinsically related to the bubble dynamics and flow pattern behavior. One may assume that these mechanisms function independently of one another for simplicity. However, the two main mechanisms may actually coexist at high vapor qualities, where the convective evaporation gradually suppresses the nucleate boiling. Therefore,

the nucleate boiling and convective evaporation contributions to the heat transfer process can be superimposed by very complex mechanisms which are not yet fully understood so far.

In particular, for micro-channels, the flow boiling mechanisms are strongly affected by the bubble behaviors in confined space and the unstable bubble dynamics [44]. From the available studies, flow boiling heat transfer mechanisms are classified into four different categories: (i) Nucleate boiling dominant because the heat transfer data are heat flux dependent; (ii) Convective boiling dominant when the heat transfer coefficient depends on mass flux and vapor quality but not heat flux; (iii) Both nucleate and convective boiling dominant, and (iv) Thin film evaporation of the liquid film around elongated bubble flows as the dominant heat transfer mechanism, which is heat flux dependent via bubble frequency and conduction across the film [44]. However, the observed flow patterns and phenomena have not yet been incorporated in the flow pattern and heat transfer prediction methods. The reduced pressure has a great effect on the flow boiling heat transfer and dryout behaviors and mechanisms. The combination effects of tube diameter, the reduced pressure, the heat flux and mass flux are very complicated but should be incorporated with the flow patterns and heat transfer model for better prediction for the heat transfer.

There is still a debate about the possible governing heat transfer mechanism for microchannel flow boiling. Generally, in the nucleate boiling dominant region, the heat transfer coefficient is mainly a function of heat flux and system pressure but is less independent of vapor quality and mass flux. In convective boiling dominant region, the heat transfer coefficient largely depends on vapor quality and mass flux but is not a function of heat flux. On this basis, many researchers have addressed their experimental flow boiling results in microchannel as governed by the nucleate boiling or the convective boiling mechanism, depending on the heat transfer coefficient trend as a function of thermal-hydraulic parameters only. In fact, the current research results are quite diverse. Some anomaly heat transfer trends cannot be explained according to the relevant heat transfer

mechanisms. For flow boiling in micro-channels, the heat transfer mechanisms should be relevant to the relevant flow regimes and bubble dynamics in micro-channels, considering the channel size effect on the bubble growth and flow patterns. Unfortunately, in most available publications, the flow patterns and flow boiling heat transfer behaviors have been separately investigated. In fact, the flow regimes and heat transfer behaviors are intrinsically related to each other. Both the flow regimes, bubble behaviors and heat transfer should be observed and measured simultaneously in experiments for a better understanding the flow boiling phenomena and mechanisms in micro-evaporators.

Furthermore, mechanistic prediction methods based on flow regimes and bubble behaviors are needed. There are several such studies available in the literature. Thome et al. [98] and Dupont et al. [99] proposed flow boiling heat transfer model based on elongated bubble flow in microscale channels, with the hypothesis that thin film evaporation is the dominant heat transfer mechanism as opposed to prior interpretations that conventional macroscale nucleate boiling dominance. Their assumption is that microscale flow is reached when the bubble growth diameter reaches the tube internal diameter followed by subsequent detachment from the wall surface. In their heat transfer model, the critical bubble radius is evaluated using the effective nucleation wall superheat. Furthermore, Consolini and Thome [100] and Thome and Cioncolini [101] have recently developed new mechanistic heat transfer model for annular flow covering both macro- and micro-channels and a flow pattern based flow boiling model for microchannel combining with the three zone model and the annular flow model. This model covers more flow regimes of elongated bubbles and annular flows which are dominant flow regimes in microchannel. Both models have been evaluated with the database by Cheng and Xia [1]. It shows very promising results with the flow pattern based heat transfer model. However, systematic knowledge and generalized prediction methods have not yet completely achieved by relating heat transfer model, mechanism and flow patterns due

to the effects of fluid types, channel sizes, test conditions and unstable flow boiling in micro-channels. In particular, generalized flow regime transition criteria are needed for developing/improving the heat transfer prediction using mechanistic methods. Effort should be made to advance systematic knowledge flow boiling heat transfer, CHF, flow regimes and the heat transfer mechanisms governing the flow boiling processes through properly designed experiments for flow boiling in both microchannels with plain surfaces and microchannels with enhanced structures in future.

## **Conclusions**

The fundamentals and challenges of flow boiling phenomena and mechanisms in micro-channel evaporators with plain surface and enhanced technologies have been reviewed and analyzed in this paper. The main conclusions are obtained as follows:

- (1) Quite different flow boiling results and mechanisms of flow boiling have been obtained by various researchers. Some studies have reported too much high heat transfer and CHF behaviors, which seem not to be true as there is limitation of the latent heat of the working fluids. Therefore, accurate experimental studies of flow boiling heat transfer, CHF and mechanisms in microchannel evaporators with plain surface are still needed. It is essential to use advanced measurement technologies specially for microscale flow boiling experiments to obtain accurate experimental data.
- (2) Flow regimes are critical to understanding the flow boiling phenomena and mechanisms in micro-channels evaporators but microscopic evolutions of bubble dynamics and flow regimes are very limited and should be focused on. In particular, they are lacking for micro-channel evaporators with enhanced technologies. Deep analysis of the results and physical mechanisms are needed by relating the heat transfer and CHF to the flow regimes.

- (3) Optimal design of microchannel evaporators with plain surface and enhanced structures is lacking. Effort should be made to achieve systematic theoretical knowledge and optimal design methods.
- (4) Flow instabilities and transient flow boiling phenomena are particularly important in understanding all aspects of flow boiling in micro-evaporators and should be focused on.
- (5) Systematic experimental, analytical and modelling studies on enhancement of flow boiling phenomena in micro-channel evaporators should be conducted to understand the physical mechanisms and develop the theoretical models. The physical mechanisms of flow boiling should be investigated based on the corresponding flow patterns and unstable and transient flow boiling and two phase flow phenomena.
- (6) The flow boiling mechanisms should be incorporated in the improvement of the models for better prediction of heat transfer coefficients and CHF at a wide range of conditions. Furthermore, effort should be made to develop mechanistic prediction methods for heat transfer and CHF by considering the flow patterns and unstable and transient two phase flow and flow boiling. Furthermore, there is no specially developed prediction methods for flow boiling in micro-evaporators with enhanced technologies, which should be explored in future.

## **Nomenclature**

$Co$	confinement number
$D_h$	hydraulic diameter, m
$e$	thickness of the microchannel base, m
$G$	mass velocity, kg/m <sup>2</sup> s
$g$	gravitational acceleration, 9.81 m/s <sup>2</sup>

$H$	height or depth of microchannel, m
$h$	heat transfer coefficient, W/m <sup>2</sup> K
$h_{tp}$	two phase heat transfer coefficient, W/m <sup>2</sup> K
$L$	length of micro-channels, m
$P_{ch}$	plain microchannels
$p$	pressure, Pa
$q$	heat flux, W/m <sup>2</sup>
$q_b$	base heat flux, W/m <sup>2</sup>
$q''_b$	base heat flux, W/m <sup>2</sup>
$q''$	heat flux, W/m <sup>2</sup>
$T$	temperature, K
$T_b$	base temperature, K
$T_{in}$	inlet temperature, K
$T_{sat}$	saturation temperature, K
$T_w$	wall temperature, K
$t$	thickness of fin in microchannel, m; time, s
$W$	width of microchannel, m
$x$	vapor quality, x coordinate
$x_e$	exit vapor quality
$y$	y coordinate

### Greek symbols

$\alpha$	heat transfer coefficient, W/m <sup>2</sup> K
----------	-----------------------------------------------

$\Delta T_{sub}$  subcooling, K

$\rho_g$  gas phase density, kg/m<sup>3</sup>

$\rho_l$  liquid phase density, kg/m<sup>3</sup>

$\sigma$  Surface tension, N/m

## Subscripts

*avionics* avionics

*b* base

*ch* microchannel

*e* exit

*g* gas phase

*h* hydraulic

*in* inlet

*l* liquid phase

*nano* nano structured

*sat* saturation

*sub* subcooled

*tp* two phase

*w* wall

*3* position 3

## Abbreviations

CHF critical heat flux, W/m<sup>2</sup>

DI Deionized

GW	groove wall
H/X	heat exchanger
IR	inlet restrictor
MEMS	micro-electro-mechanical-system
ONB	onset of nucleate boiling
PW	plain wall
RTD	resistance temperature detector
SEM	scanning electron microscope

## References

- [1] L. Cheng, and G. Xia, “Fundamental issues, mechanisms and models of flow boiling heat transfer in microscale channels,” *Int. J. Heat Mass Transfer*, vol. 108 (Part A), pp. 97-127, 2017. DOI: 10.1016/j.ijheatmasstransfer.2016.12.003.
- [2] I. Mudawar, “Assessment of high-heat-flux thermal management schemes,” *IEEE Tran. Compon. Packag. Technol.*, vol. 24, no. 2, pp. 122-141, 2001. DOI: 10.1109/6144.926375.
- [3] S. G. Kandlikar, “A roadmap for implementing minichannels in refrigeration and air-conditioning systems - current status and future directions,” *Heat Transfer Eng.*, vol. 28, no. 12, pp. 973–985, 2007. DOI: 10.1080/01457630701483497.
- [4] B. Agostini, M. Fabbri, J. E. Park, L. Wojtan, J. R. Thome, and B. Michel, “State of the art of high heat flux cooling technologies,” *Heat Transfer Eng.*, vol. 28, no. 4, pp. 258-281, 2007. DOI: 10.1080/01457630601117799
- [5] T. A. Shedd, “Next generation spray cooling: High heat flux management in compact spaces,” *Heat Transfer Eng.* Vol. 28, no. 2, pp 87-92, 2007. DOI: 10.1080/0145763060102324.

- [6] T. G. Karayiannis, and M. M. Mahmoud, “Flow boiling in microchannels: Fundamentals and applications,” *Appl. Therm. Eng.*, vol. 115, pp. 1372–1397, 2017. DOI:10.1016/j.applthermaleng.2016.08.063.
- [7] L. Cheng, “Microscale and nanoscale thermal and fluid transport phenomena: Rapidly developing research fields,” *Int. J. Microscale Nanoscale Therm. Fluid Transp. Phenom.*, vol. 1, no. 1, pp. 3-6, 2010.
- [8] S. G. Kandlikar, “Fundamental issues related to flow boiling in minichannels and microchannels,” *Exp. Therm. Fluid Sci.*, vol. 26, no. 2 - 4, pp. 389-407, 2002. DOI: 10.1016/S0894-1777(02)00150-4.
- [9] L. Cheng, “Fundamental issues of critical heat flux phenomena during flow boiling in microscale-channels and nucleate pool boiling in confined spaces,” *Heat Transfer Eng.*, vol. 34, no.13, pp. 1011-1043, 2013. DOI: doi.org/10.1080/01457632.2013.763538.
- [10] J. Lee, and I. Mudawar, “Low-temperature two-phase microchannel cooling for high-heat-flux thermal management of defense electronics,” *IEEE Tran. Compon. Packag. Technol.*, vol.. 32, no. 2, 2009, pp. 453-465. DOI: 10.1109/TCAPT.2008.2005783.
- [11] I. Mudawar, “Assessment of high-heat-flux thermal management schemes,” *IEEE Tran. Compon. Packag. Technol.*, vol. 24, no. 2, 2001. pp. 122-141. DOI: 10.1109/6144.926375.
- [12] L. Cheng, and D. Mewes, “Review of two-phase flow and flow boiling of mixtures in small and mini channels,” *Int. J. Multiphase Flow*, vol. 32, no. 2, pp. 183-207, 2006. DOI: 10.1016/j.ijmultiphaseflow.2005.10.001.
- [13] L. Cheng, G. Xia, Q. Li, and J. R. Thome, “Fundamental issues, technology development, and challenges of boiling heat transfer, critical heat flux, and two-phase flow phenomena with nanofluids,” *Heat Transfer Eng.*, vol. 40, no. 16, pp. 1301–1336, 2019. DOI: 10.1080/01457632.2018.1470285.

- [14] L. Cheng, G. Xia, and J. R. Thome, “Flow boiling heat transfer and two phase flow phenomena of CO<sub>2</sub> in macro- and micro-channel evaporators: Fundamentals, applications and engineering design,” *Appl. Therm. Eng.*, vol. 195, 170770, 2021. DOI: 10.1016/j.applthermaleng.2021.117070.
- [15] S. Szczukiewicz, M. Magnini, and J. R. Thome, “Proposed models, ongoing experiments, and latest numerical simulations of microchannel two-phase flow boiling,” *Int. J. Multiphase Flow*, vol. 59, pp. 84–101, 2014. DOI: 10.1016/j.ijmultiphaseflow.2013.10.014.
- [16] J. R. Thome, L. Cheng, G. Ribatski, and L. F. Vales, “Flow boiling of ammonia and hydrocarbons: A state-of-the-art review,” *Int. J. Refrig.*, vol. 31, no. 4, pp. 603-620, 2008. DOI: 10.1016/j.ijrefrig.2007.11.010.
- [17] Z. Guo, L. Cheng, H. Cao, H. Zhang, and X. Huang et al., “Heat transfer enhancement—A brief review of literature in 2020 and prospects,” *Heat Transfer Res.*, vol. 52, no. 10, pp. 65-92, 2021. DOI: 10.1615/HeatTransRes.2021038770.
- [18] Z. Guo, “Heat transfer enhancement – a brief review of 2018 literature,” *J. Enhanced Heat Transfer*, vol. 26, no. 5, pp. 429-449, 2019. DOI: 10.1615/JEnhHeatTransf.2019031660.
- [19] L. Cheng, E. P. Bandarra Filho, and J. R. Thome, “Nanofluid two-phase flow and thermal physics: a new research frontier of nanotechnology and its challenges,” *J. Nanosci. Nanotech.*, vol. 8, no. 7, pp. 3315-3332, 2008. DOI: 10.1166/jnn.2008.413.
- [20] Z. Guo, “A review on heat transfer enhancement with nanofluids,” *J. Enhanced Heat Transfer*, vol. 27, no. 1, pp. 1-70, 2020. DOI: 10.1615/JEnhHeatTransf.2019031575.
- [21] L. Cheng, and L. Liu, “Boiling and two phase flow phenomena of refrigerant-based nanofluids: fundamentals, applications and challenges,” *Int. J. Refrig.*, vol. 36, no. 2, pp. 421-446, 2013. DOI: 10.1016/j.ijrefrig.2012.11.010.

- [22] G. Xia, M. Du, L. Cheng, and W. Wang, "Experimental study on the nucleate boiling heat transfer characteristics of a water-based multi-walled carbon nanotubes nanofluid in a confined space," *Int. J. Heat Mass Transfer*, vol. 113, pp. 59-69, 2017. DOI: 10.1016/j.ijheatmasstransfer.2017.05.021.
- [23] L. Cheng, "Microscale flow patterns and bubble growth in microchannels," in *Microchannel Phase Change Heat Transfer*, Editor: Sujoy Kumar Saha, Elsevier Publisher, pp. 91-140. 2016. DOI: 10.1016/B978-0-12-804318-9.00003-0.
- [24] L. Cheng, "Flow boiling heat transfer with models in microchannels," in *Microchannel Phase Change Heat Transfer*, Editor: Sujoy Kumar Saha, Elsevier Publisher, pp.141-191, 2016. DOI: 10.1016/B978-0-12-804318-9.00004-2.
- [25] L. Cheng, G. Ribatski, and J. R. Thome, "Gas-liquid two-phase flow patterns and flow pattern maps: fundamentals and applications," *ASME Appl. Mech. Rev.*, vol. 61, no. 5, 50802, 2008. DOI: 10.1115/1.2955990.
- [26] P.A. Kew, and K. Cornwell, "Correlations for the prediction of boiling heat transfer in small-diameter channels," *Appl. Thermal Eng.*, vol. 17, no. 8-10, pp. 705-715, 1997. DOI: 10.1016/S1359-4311(96)00071-3.
- [27] S. S. Mehendale, A. M. Jacobi, and R. K. Shah, "Fluid flow and heat transfer at micro- and meso-scales with application to heat exchanger design," *ASME Applied Mech. Rev.*, vol. 53, no. 7, pp. 175-193. 2000. DOI: 10.1115/1.3097347.
- [28] L. Cheng, G. Ribatski, L. Wojtan, and J. R. Thome, "New flow boiling heat transfer model and flow pattern map for carbon dioxide evaporating inside horizontal tubes," *Int. J. Heat Mass Transfer*, vol. 49, no. 21-22, pp. 4082-4094, 2006. DOI: 10.1016/j.ijheatmasstransfer.2006.04.003.

- [29] L. Cheng, G. Ribatski, J. Moreno Quibén, and J. R. Thome, “New prediction methods for CO<sub>2</sub> evaporation inside tubes: Part I - A general two-phase flow pattern map and development of a phenomenological model of two-phase flow frictional pressure drop,” *Int. J. Heat Mass Transfer*, vol. 51, no. 1 - 2, pp. 111-124, 2008. DOI: 10.1016/j.ijheatmasstransfer.2012.05.044.
- [30] L. Cheng, G. Ribatski, and J. R. Thome, “New prediction methods for CO<sub>2</sub> evaporation inside tubes: Part II - A general flow boiling heat transfer model based on flow patterns,” *Int. J. Heat Mass Transfer*, vol. 51, no. 1-2, pp. 125-135, 2008. DOI: 10.1016/j.ijheatmasstransfer.2007.04.001.
- [31] J. Moreno Quibén, L. Cheng, R. J. da Silva Lima, and J. R. Thome, “Flow boiling in horizontal flattened tubes: Part I— Two-phase frictional pressure drop results and model,” *Int. J. Heat Mass Transfer*, vol. 52, no. 15–16, pp. 3634-3644, 2009. DOI: 10.1016/j.ijheatmasstransfer.2008.12.032.
- [32] J. Moreno Quibén, L. Cheng, R. J. da Silva Lima, and J. R. Thome, “Flow boiling in horizontal flattened tubes: Part II— Flow boiling heat transfer results and model,” *Int. J. Heat Mass Transfer*, vol. 52, no. 15–16, pp. 3645-3653, 2009. DOI: 10.1016/j.ijheatmasstransfer.2008.12.033.
- [33] L. Cheng, G. Xia, and Q. Li, “CO<sub>2</sub> evaporation process modelling: Fundamentals and engineering applications,” *Heat Transfer Eng.*, vol. 43, no. 8 – 10, pp. 1-28, 2022. DOI: 10.1080/01457632.2021.1905297.
- [34] L. Cheng, and G. Xia, “Flow boiling heat transfer and two-phase flow of carbon dioxide: Fundamentals, mechanistic models and applications,” *Proc. the 4th World Congr. Momentum, Heat Mass Transfer (MHMT'19)* Rome, Italy – April 10 - 12, 2019. DOI: 10.11159/icmfht19.2.

- [35] L. Cheng, and J. R. Thome, “Cooling of microprocessors using flow boiling of CO<sub>2</sub> in micro-evaporators: Preliminary analysis and performance comparison,” *Appl. Therm. Eng.*, vol. 29, no. 11 – 12, pp. 2426-2432, 2009. DOI: 10.1016/j.applthermaleng.2008.12.019.
- [36] G. R. Warrier, V. K. Dhir, and L. A. Momoda, “Heat transfer and pressure drop in narrow rectangular channels,” *Exp. Therm. Fluid Sci.*, vol. 26, no. 1, pp. 53-64, 2002. DOI: 10.1016/S0894-1777(02)00107-3.
- [37] W. Qu, and I. Mudawar, “Flow boiling heat transfer in two-phase micro-channels heat sinks – I. Experimental investigation and assessment of correlation methods,” *Int. J. Heat Mass Transfer*, vol. 46, no. 15, pp. 2755-2271, 2003. DOI: 10.1016/S0017-9310(03)00041-3.
- [38] W. Qu, and I. Mudawar, “Measurement and correlation of critical heat flux in two-phase micro-channel heat sinks,” *Int. J. Heat Mass Transfer*, vol. 47, no. 10-11, pp. 2045 -2059, 2004. DOI: 10.1016/j.ijheatmasstransfer.2003.12.006.
- [39] G. Wang, P. Cheng, and A. E. Bergles, “Effects of inlet/outlet configurations on flow boiling instability in parallel microchannels,” *Int. J. Heat and Mass Transfer*, vol. 51, no. 9-10, pp. 2267–2281, 2008. DOI: 10.1016/j.ijheatmasstransfer.2007.08.027.
- [40] J. Lee, and I. Mudawar, “Two-phase flow in high-heat-flux micro-channel heat sink for refrigeration cooling applications: Part II-heat transfer characteristics,” *Int. J. Heat Mass Transfer*, vol. 48, no. 5, pp. 941-955, 2005. DOI: 10.1016/j.ijheatmasstransfer.2004.09.018.
- [41] T. Harirchian, and S. V. Garimella, “Microchannel size effects on local flow boiling heat transfer to a dielectric fluid,” *Int. J. Heat Mass Transfer*, vol. 51, no. 15-15, 3724–3735, 2008. DOI: 10.1016/j.ijheatmasstransfer.2008.03.013.
- [42] T. Harirchian, and S. V. Garimella, “Effects of channel dimension, heat flux, and mass flux on flow boiling regimes in microchannels,” *Int. J. Multiphase Flow*, vol. 35, pp. 349–362, 2009. DOI: 10.1016/j.ijmultiphaseflow.2009.01.003.

- [43] T. Chen, and S. V. Garimella, “Measurements and high-speed visualization of flow boiling of a dielectric fluid in a silicon microchannel heat sink,” *Int. J. Multiphase Flow*, vol. 32, no. 8, pp. 957–971, 2006. DOI: 10.1016/j.ijmultiphaseflow.2006.03.002.
- [44] T. Chen, and S. V. Garimella, “Flow boiling heat transfer to a dielectric coolant in a microchannel heat sink,” *IEEE Trans. Compon. Packag. Technol.*, vol. 30, no. 1, pp. 24–31, 2006. DOI: 10.1109/TCAPT.2007.892063
- [45] G. Hetsroni, A. Mosyak, Z. Segal, and G. Ziskind, “A uniform temperature heat sink for cooling of electronic devices,” *Int. J. Heat Mass Transfer*, vol. 45, no. 16, pp. 3275-3286, 2002. DOI: 10.1016/S0017-9310(02)00048-0.
- [46] L. Jiang, M. Wong, and Y. Zohar, “Phase change in microchannel heat sinks with integrated temperature sensors,” *J. Microelectromech. Syst.*, vol. 8, no. 4, pp. 358-365, 1999. DOI: 10.1109/84.809049.
- [47] Y. K. Prajapati and P. Bhandari, “Flow boiling instabilities in microchannels and their promising solutions – A review,” *Exp. Therm. Fluid Sci.*, vol. 88, pp. 576–593, 2017. DOI: 10.1016/j.expthermflusci.2017.07.014.
- [48] G. Ribatski, L. Wojtan and J.R. Thome, “An analysis of experimental data and prediction methods for two-phase frictional pressure drop and flow boiling heat transfer in micro-scale channels,” *Exp. Therm. Fluid Sci.*, vol. 31, no. 1, 2006, pp. 1-19, 2006. DOI: 10.1016/j.expthermflusci.2006.01.006.
- [49] C.B. Tibirica and G. Ribatski, “Flow boiling in micro-scale channels – Synthesized literature review,” *Int. J. Refrig.*, vol. 36, no. 2, pp. 301-324, 2013. DOI: 10.1016/j.ijrefrig.2012.11.019.
- [50] S. Lee, and I. Mudawar, “Investigation of flow boiling in large micro-channel heat exchangers in a refrigeration loop for space applications,” *Int. J. Heat Mass Transfer*, vol. 97, pp. 110–129, 2016. DOI: 10.1016/j.ijheatmasstransfer.2016.01.072.

- [51] B. Agostini, J. R. Thome, M. Fabbri, B. Michel, and D. Calmi et al., “High heat flux flow boiling in silicon multi-microchannels – Part I: Heat transfer characteristics of refrigerant R236fa,” *Int. J. Heat Mass Transfer*, vol. 51, no. 21-22, pp. 5400–5414, 2008. DOI:10.1016/j.ijheatmasstransfer.2008.03.006.
- [52] B. Agostini, J. R. Thome, M. Fabbri, B. Michel, and D. Calmi et al., “High heat flux flow boiling in silicon multi-microchannels – Part II: Heat transfer characteristics of refrigerant R245fa,” *Int. J. Heat Mass Transfer*, vol. 51, no. 21-22, pp. 5415–5425, 2008. DOI: 10.1016/j.ijheatmasstransfer.2008.03.007
- [53] B. Agostini, R. Revellin, J. R.; Thome, M. Fabbri, and B. Michel et al., “High heat flux flow boiling in silicon multi-microchannels – Part III: Saturated critical heat flux of R236fa and two-phase pressure drops,” *Int. J. Heat Mass Transfer*, vol. 51, no. 21-22, pp. 5426–5442, 2008. DOI: 10.1016/j.ijheatmasstransfer.2008.03.005.
- [54] J. Park, and J. R. Thome, “Critical heat flux in multi-microchannel copper elements with low pressure refrigerants,” *Int. J. Heat Mass Transfer*, vol. 53, no. 1-3, pp. 110–122, 2010. DOI: 10.1016/j.ijheatmasstransfer.2009.09.047.
- [55] A.W. Mauro, J.R. Thome, D. Toto, and G.P. Vanoli, “Saturated critical heat flux in a multi-microchannel heat sink fed by a split flow system,” *Exp. Therm. Fluid Sci.*, vol. 34, no.1, pp. 81–92, 2010. Doi: 10.1016/j.expthermflusci.2009.09.005.
- [56] S. Lee, and I. Mudawar, “Transient characteristics of flow boiling in large micro-channel heat exchangers,” *Int. J. Heat Mass Transfer*, vol. 103, pp. 186–202, 2016. Doi:10.1016/j.ijheatmasstransfer.2016.07.040.
- [57] S. Lee, V.S. Devahdhanush, and I. Mudawar “Investigation of subcooled and saturated boiling heat transfer mechanisms, instabilities, and transient flow regime maps for large length-

to-diameter ratio micro-channel heat sinks,” *Int. J. Heat Mass Transfer*, vol 123, pp. 172–191, 2018. DOI: 10.1016/j.ijheatmasstransfer.2018.02.020.

[58] H. Huang, and J.R. Thome, “Local measurements and a new flow pattern based model for subcooled and saturated flow boiling heat transfer in multi-microchannel evaporators,” *Int. J. Heat Mass Transfer*, vol. 103, pp. 701-714, 2016. DOI: 10.1016/j.ijheatmasstransfer.2016.07.074.

[59] H. Huang, L. Pan, and R. Yan, “Flow characteristics and instability analysis of pressure drop in parallel multiple microchannels,” *Appl. Therm. Eng.*, vol. 142, pp. 184–193, 2018. DOI: 10.1016/j.applthermaleng.2018.06.083.

[60] E.M. Fayyadh, M.M. Mahmoud, K. Sefiane, and T.G. Karayiannis, “Flow boiling heat transfer of R134a in multi microchannels,” *Int. J. Heat Mass Transfer*, vol. 110, pp. 422–436, 2017. DOI: 10.1016/j.ijheatmasstransfer.2017.03.057.

[61] Y. Lv, G. Xia, L Cheng, and D. Ma, “Experimental investigation into unstable two phase flow phenomena during flow boiling in multi-microchannels,” *Int. J. Therm. Sci.*, vol. 166, 106985, 2021. DOI: 10.1016/j.ijthermalsci.2021.106985.

[62] G. Xia, Y. Lv, L. Cheng, D. Ma, and Y. Jia, “Experimental study and dynamic simulation of the continuous two phase instable boiling in multiple parallel microchannels,” *Int. J. Heat Mass Transfer*, vol. 138, pp. 961-984, 2019. DOI: 10.1016/j.ijheatmasstransfer.2019.04.124.

[63] Y. Lv, G. Xia, L. Cheng, and D. Ma, “Experimental study on the pressure drop oscillation characteristics of the flow boiling instability with FC-72 in parallel rectangle microchannels,” *Int. Comm. Heat Mass Transfer*, vol. 108, 104289, 2019. DOI: 10.1016/j.icheatmasstransfer.2019.104289.

- [64] M. R. Özdemir, M. M. Mahmoud, and T.G. Karayiannis, “Flow Boiling of water in a rectangular metallic microchannel,” *Heat Transfer Eng.*, vol. 42, no. 6, pp. 492-516, 2019. DOI: 10.1080/01457632.2019.1707390.
- [65] G. Hedau, P. Dey, R. Raj, and S. K. Saha, “Combined effect of inlet restrictor and nanostructure on two-phase flow performance of parallel microchannel heat sinks,” *Int. J. Therm. Sci.*, vol. 153, 106339, 2020. DOI: 10.1016/j.ijthermalsci.2020.106339.
- [66] R. Diaz, and Z. Guo, “Enhanced conduction and pool boiling heat transfer on single-layer graphene-coated substrates,” *J. Enhanced Heat Transfer*, vol. 26, no. 2, pp. 127-143, 2019. DOI: 10.1615/JEnhHeatTransf.2018028488.
- [67] S. K. Nayak, and P. C. Mishra, “Enhanced heat transfer from hot surface by nanofluid based ultrafast cooling: an experimental investigation,” *J. Enhanced Heat Transfer*, vol. 26, no. 4, pp. 415-428, 2019. DOI: 10.1615/JEnhHeatTransf.2019028238.
- [68] H. Kubo, H. Takamatsu, and H. Honda, “Effects of size and number density of micro-reentrant cavities on boiling heat transfer from a silicon chip immersed in degassed and gas-dissolved FC-72,” *J. Enhanced Heat Transfer*, vol. 6, no. 2-4, pp. 151-160, 1999. DOI: 10.1615/JEnhHeatTransf.v6.i2-4.80.
- [69] H. Honda, H. Takamatsu, and J. J. Wei, “Enhanced boiling heat transfer from silicon chips with micro-pin fins immersed in FC-72,” *J. Enhanced Heat Transfer*, vol. 10, no. 2, pp. 211-224, 2003. DOI: 10.1615/JEnhHeatTransf.v10.i2.70.
- [70] U. Sajjad, A. Kumar, and Chi-Chuan Wang, “Nucleate pool boiling of sintered coated porous surfaces with dielectric liquid, HFE-7200,” *J. Enhanced Heat Transfer*, vol. 27, no. 8, pp. 767-784, 2020. DOI: 10.1615/JEnhHeatTransf.2020035315.

- [71] V. V. Nirgude, and S. K. Sahu, “Nucleate boiling heat transfer performance of laser textured copper surfaces,” *J. Enhanced Heat Transfer*, vol. 26, no. 6, pp. 597-618, 2019. DOI: 10.1615/JEnhHeatTransf.2019030631.
- [72] M. Piasecka, and K. Strąk, “Influence of the Surface Enhancement on the Flow Boiling Heat Transfer in a Minichannel,” *Heat Transfer Eng.*, vol. 40, no. 13-14, pp. 1162-1175, 2019. DOI: 10.1080/01457632.2018.1457264.
- [73] R. Hoke, B. E. Burk, J. Kotovsky, J. Hamilton, and P. Fontejon et al. “High flux boiling heat transfer enhancement using triangle shaped vertical walls in two-phase microchannel heat exchangers,” *Heat Transfer Res.*, vol. 52, no. 7, pp. 1-16, 2021. DOI: 10.1615/HeatTransRes.2021035809
- [74] L. Cheng, and T. Chen, “Study of flow boiling heat transfer in a tube with axial microgrooves,” *Exp. Heat Transfer*, vol.14, no. 1, pp. 59-73, 2001. DOI: 10.1080/089161501461648.
- [75] D. Deng, L. Zeng, and W. Sun, “A review on flow boiling enhancement and fabrication of enhanced microchannels of microchannel heat sinks,” *Int. J. Heat Mass Transfer*, vol. 175, 121332, 2021. DOI: 10.1016/j.ijheatmasstransfer.2021.121332.
- [76] Y. Li, G. Xia, Y. Jia, Y. Cheng, and J. Wang, “Experimental Investigation of flow boiling performance in microchannels with and without triangular cavities – A comparative study,” *Int. J. Heat Mass Transfer*, vol. 108, Part B, 1511–1526, 2017. DOI: 10.1016/j.ijheatmasstransfer.2017.01.011.
- [77] Y.F. Li, G.D. Xia, D.D. Ma, J.L. Yang, and W. Li, “Experimental investigation of flow boiling characteristics in microchannel with triangular cavities and rectangular fins,” *Int. J. Heat Mass Transfer*, vol. 148, 119036, 2020. DOI: 10.1016/j.ijheatmasstransfer.2019.119036.

- [78] J. Xu, X. Yu, and W. Jin, "Porous-wall microchannels generate high frequency "eye-blinking" interface oscillation, yielding ultra-stable wall temperatures," *Int J Heat Mass Transfer*, vol 101 pp. 341–353, 2016. DOI: 10.1016/j.ijheatmasstransfer.2016.05.039.
- [79] Y.T. Jia, G.D. Xia, L.X. Zong, D.D. Ma, and Y.X. Tang, "A comparative study of experimental flow boiling heat transfer and pressure drop characteristics in porous-wall microchannel heat sink," *Int J Heat Mass Transfer*, vol. 127, Part A, pp. 818–833, 2018. DOI: 10.1016/j.ijheatmasstransfer.2018.06.090
- [80] G. Xia, Y. Cheng, L. Cheng, and Y. Li, "Heat transfer characteristics and flow visualization during flow boiling of acetone in semi-open multi-microchannels," *Heat Transfer Eng.*, vol. 40, no. 16, pp. 1349-1362, 2019. DOI: 10.1080/01457632.2018.1470296.
- [81] L.X. Zong, G.D. Xia, Y.T. Jia, L. Liu and D.D. Ma et al., "Flow boiling instability characteristics in microchannels with porous-wall," *Int. J. Heat Mass Transfer*, vol. 146, 118863, 2020. DOI: 10.1016/j.ijheatmasstransfer.2019.118863.
- [82] X. Cheng and H. Wu, "Enhanced flow boiling performance in high-aspect-ratio groove-wall microchannels," *Int. J. Heat Mass Transfer*, vol. 164, 120468, 2021. DOI: 10.1016/j.ijheatmasstransfer.2020.120468
- [83] C. Ren, W. Li, J. Ma, G. Huang, and C. Li, "Flow boiling in microchannels enhanced by parallel microgrooves fabricated on the bottom surfaces," *Int. J. Heat Mass Transfer*, vol. 166, 120756, 2021. DOI: 10.1016/j.ijheatmasstransfer.2020.120756.
- [84] Q. Zhao, J. Qiu, J. Zhou, M. Lu, and Q. Li et al., "Visualization study of flow boiling characteristics in open microchannels with different wettability," *Int. J. Heat Mass Transfer*, vol. 180, 121808, 2021. DOI: 10.1016/j.ijheatmasstransfer.2021.121808.

- [85] W. Li, J. Ma, T. Alam, F. Yang, and J. Khan, “Flow boiling of HFE-7100 in silicon microchannels integrated with multiple micro-nozzles and reentry micro-cavities,” *Int. J. Heat Mass Transfer*, vol.123, pp. 354–366, 2018. DOI: 10.1016/j.ijheatmasstransfer.2018.02.108.
- [86] W. Li, C. Li, Z. Wang, and Y. Chen “Enhanced flow boiling in microchannels integrated with supercapillary pinfin fences,” *Int. J. Heat Mass Transfer*, vol. 183, 122185, 2022. DOI: 10.1016/j.ijheatmasstransfer.2021.122185.
- [87] D. Deng, L. Chen, W. Wan, T. Fu, and X. Huang, “Flow boiling performance in pin fin-interconnected reentrant microchannels heat sink in different operational conditions,” *Appl. Therm. Eng.*, vol. 150, pp. 1260–1272, 2019. DOI: 10.1016/j.applthermaleng.2019.01.092
- [88] D. Deng, Y. Xie, Q. Huang, Y. Tang, and L. Huang et al., “Flow boiling performance of  $\Omega$ -shaped reentrant copper microchannels with different channel sizes,” *Exp. Therm. Fluid Sci.*, vol. 69, pp. 8-18, 2015. doi.org/10.1016/j.expthermflusci.2015.07.016
- [89] Y. K. Prajapati, M. Pathak, and M. K.Khan, “Bubble dynamics and flow boiling characteristics in three different microchannel configurations,” *Int. J. Therm. Sci.*, vol. 112, pp. 371-382, 2017. DOI: 10.1016/j.ijthermalsci.2016.10.021.
- [90] A. Koşar, C. Kuo, and Y. Peles, “Boiling heat transfer in rectangular microchannels with reentrant cavities,” *Int. J. Heat Mass Transfer*, vol. 48, no. 23-24, pp. 4867-4886, 2005. DOI: 10.1016/j.ijheatmasstransfer.2005.06.003.
- [91] C.J. Kuo, and Y. Peles, “Local measurement of flow boiling in structured surface microchannels,” *Int. J. Heat Mass Transfer*, vol. 50, no. 23-24, pp. 4513-4526, 2007. DOI: 10.1016/j.ijheatmasstransfer.2007.03.047.

- [92] A Sitar, and I. Golobic, “Heat transfer enhancement of self-rewetting aqueous n-butanol solutions boiling in microchannels,” *Int. J. Heat Mass Transfer*, vol. 81, pp. 198-206, 2015. DOI: doi.org/10.1016/j.ijheatmasstransfer.2014.10.034.
- [93] W. Li, X. Qu, T. Alam, F. Yang, W. Chang, J. Khan, and C. Li, “Enhanced flow boiling in microchannels through integrating multiple micro-nozzles and reentry microcavities,” *Appl. Phys. Lett.*, vol. 110, 14104, 2017. DOI: 10.1063/1.4973495.
- [94] L. Cheng, and T. Cheng, “Comparison of six typical correlations for upward flow boiling heat transfer with kerosene in a vertical smooth tube,” *Heat Transfer Eng.*, vol. 21, no. 5, pp. 27-34, 2000. DOI: 10.1080/01457630050127928.
- [95] L. Cheng, and H. Zou, “Evaluation of flow boiling heat transfer correlations with experimental data of R134a, R22, R410A and R245fa in microscale channels,” *Int. J. Microscale Nanoscale Therm. Fluid Transp. Phenom.*, vol. 1, no. 4, pp. 363-380, 2010.
- [96] S-M. Kim, and I. Mudawar, “Review of databases and predictive methods for heat transfer in condensing and boiling mini/micro-channel flows,” *Int. J. Heat and Mass Transfer*, vol. 77, pp. 627–652, 2014. DOI: 10.1016/j.ijheatmasstransfer.2014.05.036.
- [97] J. C. Chen, “Correlation for boiling heat transfer to saturated fluids in convective flow,” *Ind. Eng. Chem. Process Des. Dev.*, vol. 5, no. 3, pp. 322 -329, 1966. DOI: 10.1021/i260019a023.
- [98] J. R. Thome, V. Dupont, and A. M. Jacobi, “Heat transfer model for evaporation in microchannels. Part I: Presentation of the model,” *Int. J. Heat Mass Transfer*, vol. 47, no. 14-16, pp. 3375–3385, 2004. DOI: 10.1016/j.ijheatmasstransfer.2004.01.006.
- [99] V. Dupont, J. R. Thome, and A. M. Jacobi, “Heat transfer model for evaporation in microchannels. Part II: Comparison with the database,” *Int. J. Heat Mass Transfer*, vol. 47, no. 14-16, pp. 3387–3401, 2004. DOI: 10.1016/j.ijheatmasstransfer.2004.01.007.

- [100] A. Cioncolini, and J.R. Thome, “Algebraic Turbulence Modeling in Adiabatic and Evaporating Annular Two- Phase Flow,” *Int. J. Heat Fluid Flow*, vol. 32, no. 4, pp. 805–817, 2011. DOI: 10.1016/j.ijheatfluidflow.2011.05.006.
- [101] J. R. Thome, and A. Cioncolini, “Unified model suite for two phase flow, convective boiling and condensation in macro- and microchannel,” *Heat Transfer Eng.*, vol. 37, no. 13-14, pp. 1148-1157, 2016. DOI: 10.1080/01457632.2015.1112212

Table 1. Selected studies on flow boiling heat transfer, CHF, mechanisms and two phase instabilities in conventional microscale channels with plain surface in the literature.

Authors	Fluid	Parameter ranges G (kg/m <sup>2</sup> s), q (kW/m <sup>2</sup> ), T (°C)/P (bar)	Channel size D <sub>h</sub> (mm), Geometry and orientation	Research contents
Lee and Mudawar [50]	R-134a	G = 152.90– 530.72 kg/m <sup>2</sup> s q <sub>b</sub> = 8072.93– 48,437.60 W/m <sup>2</sup> T <sub>sat</sub> = -3.59-19.41°C	D <sub>h</sub> = 1 mm, 75 and 100 parallel rectangular channels, horizontal	Flow boiling heat transfer, flow regimes and heat transfer mechanisms
Agostini et al. [51-53]	R236fa, R245fa	G= 281 to 1501 kg/m <sup>2</sup> s q <sub>b</sub> = 3.6 to 221 W/cm <sup>2</sup> , T <sub>sat</sub> = 25°C	67 parallel channels, which are 223 μm wide, 680 μm high and 20 mm long with 80 μm thick fin, horizontal	Flow boiling heat transfer, CHF and two phase pressure drop
Park and Thome [54]	R134a, R236fa, R245fa	G = 100 to 4000 kg/m <sup>2</sup> s q <sub>b</sub> = 37 to 342 W/cm <sup>2</sup> , T <sub>sat</sub> = 10 to 50°C	20 parallel rectangular channels, 467 μm wide and 4052 μm deep while the sec- and has 29 channels, 199 μm wide and 756 μm deep, horizontal	Saturated CHF
Mauro et al. [55]	R134a, R236fa, R245fa	G = 250 to 1500 kg/m <sup>2</sup> s, q <sub>b</sub> = 37 to 342 W/cm <sup>2</sup> , T <sub>sat</sub> = 20 to 50, Subcooled -25 to -5	29 parallel channels that were 199 μm wide and 756 μm deep, horizontal	Saturated CHF and effect of inlet subcooling of CHF
Lee and Mudawar [56]	R134a	G = 152.90 – 530.72 kg/m <sup>2</sup> s, q <sub>b</sub> = 8072.93 – 48,437.60 W/m <sup>2</sup> , T <sub>sat</sub> = -3.59-19.41°C	D <sub>h</sub> = 1 mm, 75 and 100 parallel rectangular channels, horizontal	Flow boiling instability and flow regime transitions

Lee et al. [57]	R134a	$G = 75.92\text{--}208.79$ $\text{kg/m}^2 \text{ s}$ , $p_{\text{in}} = 688.3\text{--}731.3$ $\text{kPa}$ , $q_b = 3990\text{--}28,209$ $\text{W/m}^2$	$D_h = 1$ mm, 100 parallel rectangular channels, horizontal	Subcooled and saturated flow boiling heat transfer, instabilities and flow regimes.
Huang and Thome [58]	R245fa, R236fa, R1233z d(E)	$G = 1250$ to $2750$ $\text{kg}/(\text{m}^2 \cdot \text{s})$ , $q = 20$ to $64$ $\text{W}/\text{cm}^2$ , $T_{\text{sat}} = 1.5, 35$ and $40^\circ\text{C}$	67 channels. Each etched channel was $100$ $\mu\text{m}$ in height, $100$ $\mu\text{m}$ in width, horizontal	Flow boiling heat transfer
Huang et al. [59]	Deionized water	$G = 23.04\text{--}111.89$ $\text{kg}/(\text{m}^2 \text{ s})$ , $q = 4.2\text{--}67.7$ $\text{kW/m}^2$ , $T_{\text{in}} = 40\text{--}60$ $^\circ\text{C}$	$D_h = 517$ $\mu\text{m}$ , 6 parallel rectangular channels, horizontal	Flow boiling dynamic instability
Fayyadh et al. [60]	R134a	$G = 50\text{--}300$ $\text{kg/m}^2$ , $q = 11.46\text{--}403.1$ $\text{kW/m}^2$ , $p = 6.5$ bar	$D_h = 420$ $\mu\text{m}$ , 25 rectangular microchannels, horizontal	Flow boiling heat transfer, flow patterns.
Lv et al. [61]	HFE-7100	$G = 380$ to $3500$ $\text{kg/m}^2 \text{ s}$ , $q = 0$ to $100$ $\text{kW/m}^2$ , $T_{\text{sat}} = 61^\circ\text{C}$	$D_h = 84.1$ $\mu\text{m}$ and $106$ $\mu\text{m}$ , 8 rectangular microchannels, horizontal	Unstable flow boiling and two phase flow.
Xia et al. [62]	Acetone	$G = 437.2$ to $868.1$ $\text{kg/m}^2 \text{ s}$ , $q = 0$ to $100$ $\text{kW/m}^2$ , $T_{\text{sat}} = 56.29^\circ\text{C}$	$D_h = 104.3$ $\mu\text{m}$ , 16 rectangular microchannels, horizontal	Unstable flow boiling and two phase flow.
Lv et al. [63]	FC-72	$G = 578.2$ to $2310.9$ $\text{kg/m}^2 \text{ s}$ , $q = 0$ to $1200$ $\text{kW/m}^2$ , $T_{\text{sat}} = 56.5^\circ\text{C}$	$D_h = 88$ $\mu\text{m}$ , 8 rectangular microchannels, horizontal	Pressure drop oscillation characteristics of the flow boiling instability.

Table 2. Selected studies on enhancement of flow boiling heat transfer and CHF in microchannel evaporators in the literature.

Authors	Fluid	Parameter ranges G (kg/m <sup>2</sup> s), q (kW/m <sup>2</sup> ), T (°C)/P (bar)	Channel size D <sub>h</sub> (mm), Substrate, Geometry,)	Research contents
Li et al. [76, 77]	Acetone	G = 83 and 442 kg/m <sup>2</sup> q = 0 - 101 W/cm <sup>2</sup> T <sub>sat</sub> = 56.29 °C	200 μm in width and 200 μm in depth 14 microchannels with triangular cavities and rectangular fins	Flow boiling heat transfer and CHF enhancement
Xu et al. [78]	Acetone	G = 154–276 kg/m <sup>2</sup> s, q = 27.22–227.05 kW/m <sup>2</sup> T <sub>sat</sub> = 56.29 °C	depth was 75 μm. A bare channel and a porous wall had a width of 164 μm and 336 μm	Flow boiling instability.
Jia et al. [79]	Acetone	G = 255 - 843 kg/m <sup>2</sup> s, q = 4 - 110 W/cm <sup>2</sup> T <sub>sat</sub> = 56.29 °C	16 microchannels height of 80 μm with a width of 150 μm	Flow boiling heat transfer and CHF enhancement
Xia et al. [80]	Acetone	G = 4.43 to 15.62 kg/(m <sup>2</sup> s), q = 0 to 90 kW/m <sup>2</sup> T <sub>sat</sub> = 56.29 °C	19 straight and semi-open microchannels height of 0.80 mm with a width of 1 mm	Flow boiling heat transfer enhancement
Zong et al. [81]	Acetone	G = 250–510 kg/m <sup>2</sup> s, q = 120–720 kW/m <sup>2</sup> T <sub>sat</sub> = 56.29 °C	16 porous-wall microchannels height of 80 μm with a width of 150 μm	Flow boiling instability.
Cheng and Wu [82]	Deionized water	G = 446, 630 and 815 kg/m <sup>2</sup> s, q <sub>w</sub> = 3.8–139.5 W/cm <sup>2</sup> T <sub>sat</sub> = 100 °C	14 parallel microchannels width and depth 80 μm × 200 μm	Flow boiling heat transfer and CHF enhancement, two phase pressure drop.

Ren et al. [83]	Water	$G = 100$ to $600 \text{ kg/m}^2\text{s}$ $q = 0$ – $400 \text{ W/cm}^2$ $T_{\text{sat}} = 100 \text{ }^\circ\text{C}$	5 rectangular parallel microchannels ( $W=200 \text{ }\mu\text{m}$ , $H=250 \text{ }\mu\text{m}$ , $L=10 \text{ mm}$ ) with microgrooves	Flow boiling heat transfer and CHF enhancement
Zhao et al. [84]	Water	$G = 172$ to $382 \text{ kg/m}^2\text{s}$ $q = 261.8$ – $597.9 \text{ kW/m}^2$ $T_{\text{sat}} = 100 \text{ }^\circ\text{C}$	16 parallel $0.3 \text{ mm} \times 0.3 \text{ mm}$ open microchannels with superhydrophilic hydrophilic and superhydrophobic	Flow boiling heat transfer, flow regimes and two phase pressure drop
Li et al. [85]	DI-water and HFE-7100	$G = 80$ to $600 \text{ kg/m}^2\text{s}$ $q$ is up to $944 \text{ W/cm}^2$ $T_{\text{sat}} = 100 \text{ }^\circ\text{C}$ (water) $T_{\text{sat}} = 61 \text{ }^\circ\text{C}$ (HFE-7100)	5 microchannels $W = 200 \text{ }\mu\text{m}$ , $H = 250 \text{ }\mu\text{m}$ by incorporating capillary micro-pinfin fences and multiple micro-nozzles	Flow boiling heat transfer and CHF enhancement
Li et al. [86]	DI water and HFE-7100	$G = 80$ to $389 \text{ kg/m}^2\text{s}$ $q$ is up to $944 \text{ W/cm}^2$ $T_{\text{sat}} = 100 \text{ }^\circ\text{C}$ (water) $T_{\text{sat}} = 61 \text{ }^\circ\text{C}$ (HFE-7100)	5 microchannels $W = 200 \text{ }\mu\text{m}$ , $H = 250 \text{ }\mu\text{m}$ by incorporating supercapillary micro-pinfin fences	Flow boiling heat transfer and CHF enhancement
Deng et al. [87]	DI water and ethanol	$G = 125$ – $300 \text{ kg/m}^2\text{s}$ $T_{\text{sat}} = 100 \text{ }^\circ\text{C}$ (water) $T_{\text{sat}} = 78^\circ\text{C}$ Inlet subcoolings of $40 \text{ }^\circ\text{C}$ and $10 \text{ }^\circ\text{C}$	Pin fin-interconnected reentrant microchannels	Flow boiling heat transfer, pressure drop and two-phase flow instabilities
Deng et al. [88]	DI-water	$G = 125$ – $300 \text{ kg/m}^2\text{s}$ $T_{\text{sat}} = 100 \text{ }^\circ\text{C}$ Inlet subcoolings of $40 \text{ }^\circ\text{C}$ and $10 \text{ }^\circ\text{C}$	Three reentrant copper microchannels with different hydraulic diameters, i.e., $590$ , $781$ and $858 \text{ }\mu\text{m}$	Flow boiling heat transfer, pressure drop and two-phase flow instabilities
Prajapati et al. [89]	DI-water	$G = 100$ to $350 \text{ kg/m}^2\text{s}$ $q = 10$ to $350 \text{ kW/m}^2$ $T_{\text{sat}} = 100 \text{ }^\circ\text{C}$	12 microchannels with $522 \text{ }\mu\text{m} \times 400 \text{ }\mu\text{m}$ and depth of $750 \text{ }\mu\text{m}$ (uniform and diverging segmented fins)	Flow boiling bubble dynamics and instability

## List of Figure Captions

Figure 1. Silicon test die photographs: Top: multi-microchannel. Bottom: (a) cobra heater, (b) connectors for one RTD (Resistance Temperature Detector), (c) the five RTDs by Agostini e al. [51].

Figure 2. Scanning electron microscope photograph of the multi-micro-channels at three different scales. The middle and bottom figures are close-ups of the fin wall by Agostini e al. [51].

Figure 3. (a) Schematic diagram of a silicon multi-microchannel evaporator used for chips cooling; (b) Comparisons of simulation results of base temperature of CO<sub>2</sub> and R236fa at the indicated conditions for chips cooling by Cheng and Thome [35].

Figure 4. Measured local flow boiling heat transfer coefficient versus local vapour quality for various mass velocities, for the base heat fluxes of 37.7 (a) and 103.3 W/cm<sup>2</sup> (b) by Agostini et al. [52].

Figure 5. Heat transfer trends identified in the study for R245fa and R236fa: the arrows show the effect of the parameters heat flux  $q$ , vapor quality  $x$  and mass flux  $G$  on heat transfer coefficient  $\alpha$ , either increasing ( $\nearrow$ ), decreasing ( $\searrow$ ) or no effect ( $\rightarrow$ ) on  $\alpha$  by Agostini et al. [52].

Figure 6. Experimental base CHF results for R134a at  $T_{\text{sat}} = 25^\circ\text{C}$  in the microchannel evaporator with deep  $H = 4052 \mu\text{m}$  channels by Park and Thome [54].

Figure 7. Experimental base CHF results for R134a at  $T_{\text{sat}} = 25^\circ\text{C}$  in the microchannel evaporator with deep  $H = 765 \mu\text{m}$  channels by Park and Thome [54].

Figure 8. (a) Variation of heat transfer coefficient with axial distance in avionics  $H/X$  at  $G_{\text{avionics}} = 340.23 \text{ kg/m}^2 \text{ s}$  and  $q_{\text{avionics}} = 44,401.1 \text{ W/m}^2$ . (b) Schematics of flow boiling for the quality ranges in (a) illustrating dominant flow patterns and heat transfer mechanisms by Lee and Mudawar [50].

Figure 9. Major causes of flow boiling instabilities in microchannels by Prajapati and Bhandari [47].

Figure 10. Schematic renderings of transient flow patterns observed at six different times within a single periodic cycle:  $t_1$ : beginning of the cycle,  $t_2$ : forward liquid advance,  $t_3$ : rapid bubble growth,  $t_4$ : commencement of transition pattern,  $t_5$ : commencement of wavy annular pattern, and  $t_6$ : end of liquid deficient period. The indicated sections are as follows: 1: subcooled boiling dominant, 2: combined saturated nucleate and convective boiling, 3: saturated convective boiling by annular film evaporation, and 4: intermittent dryout dominant region by Lee et al. [57].

Figure 11. Temporal variation of pressure drop at (a) heat flux of  $81 \text{ W/cm}^2$  and mass velocity of  $250 \text{ kg/m}^2\text{s}$  and (b) heat flux of  $137 \text{ W/cm}^2$  and mass velocity of  $250 \text{ kg/m}^2\text{s}$ , (c) heat flux of  $81 \text{ W/cm}^2$  and mass velocity of  $500 \text{ kg/m}^2\text{s}$  and (d) heat flux of  $137 \text{ W/cm}^2$  and mass velocity of  $500 \text{ kg/m}^2\text{s}$  by Hedau et al. [65].

Figure 12. Fluctuations of the surface temperature at (a) heat flux of  $81 \text{ W/cm}^2$  and (b) heat flux  $137 \text{ W/cm}^2$  and fluctuations of mass velocity at (c) heat flux of  $81 \text{ W/cm}^2$  and (d) heat flux of  $137 \text{ W/cm}^2$  for mass velocity of  $250 \text{ kg/m}^2\text{s}$  by Hedau et al. [65].

Figure 13. SEM images of (a) gradient-porous-wall microchannel [52], (b) microchannels with gradient micro pin fins [53]. (c) rectangular porous-wall microchannel with uniform circular pin fins [54] by Deng et al. [73].

Figure 14. Microscopic images of microchannels with (a) interconnected reentrant cavities [83], (b) nonconnected reentrant cavity [85], (c) different shaped reentrant cavities [89], (d) reentrant microcavities on the sidewall [90] by Deng et al. [73].

Figure 15. (a) Design of the microchannel heat sink; (b) Detailed parameters of the two microchannels by Cheng and Wu [82].

Figure 16. Typical V-shaped heat transfer coefficient curves for the microchannels with plain wall (PW) and groove wall (GW). The effective heat transfer coefficients are depicted versus (a) the effective heat flux and (b) the exit vapor quality (working fluid of DI-water) by Cheng and Wu [82].

Figure 17. Development of conceptualization. (a) The SEM image of plain wall, (b) a SEM image of micro-pinfin fences, (c) the top-view of the receding liquid profile on the smooth wall and the one on the wall with micro-pinfin fences (re-colored image, blue represents liquid of water) and, (d) schematic of the thin film evaporation within micro-pinfin fence by Li et al. [86].

Figure 18. Boiling curves plotted with base heat flux (a)  $\Delta T_{\text{sub}}=70$  °C and (b)  $\Delta T_{\text{sub}}=40$  °C by Li et al. [86].

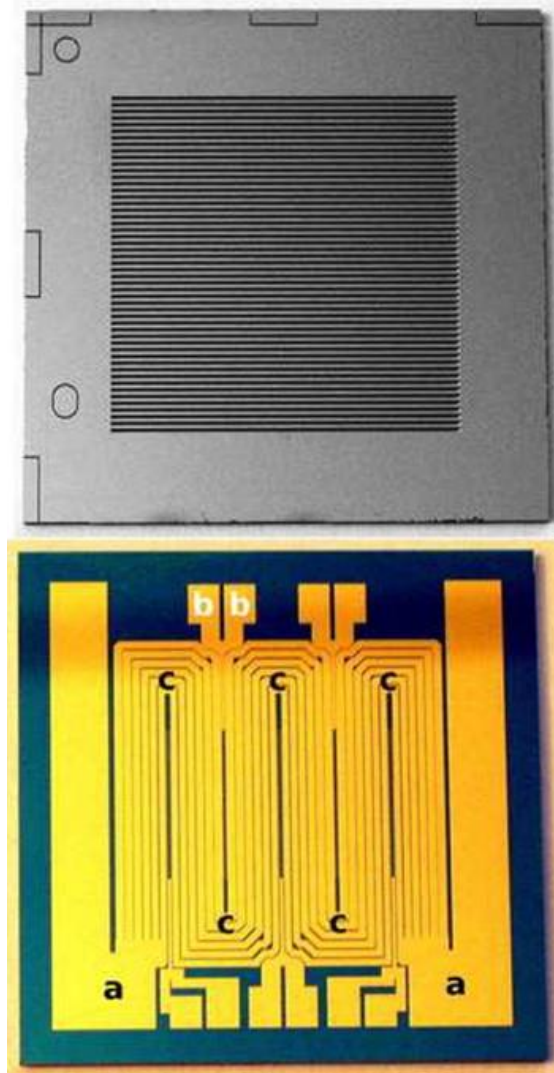


Figure 1. Silicon test die photographs: Top: multi-microchannel. Bottom: (a) cobra heater, (b) connectors for one RTD (Resistance Temperature Detector), (c) the five RTDs by Agostini e al. [51].

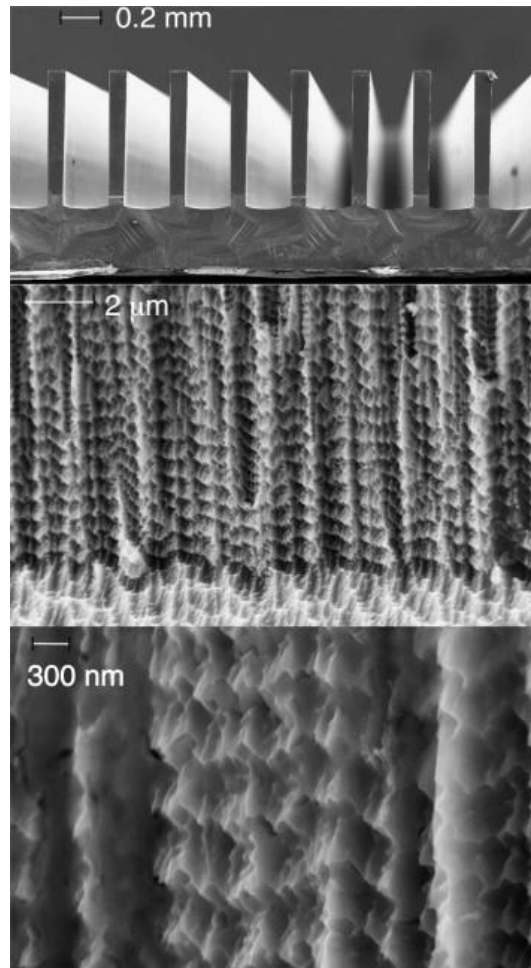
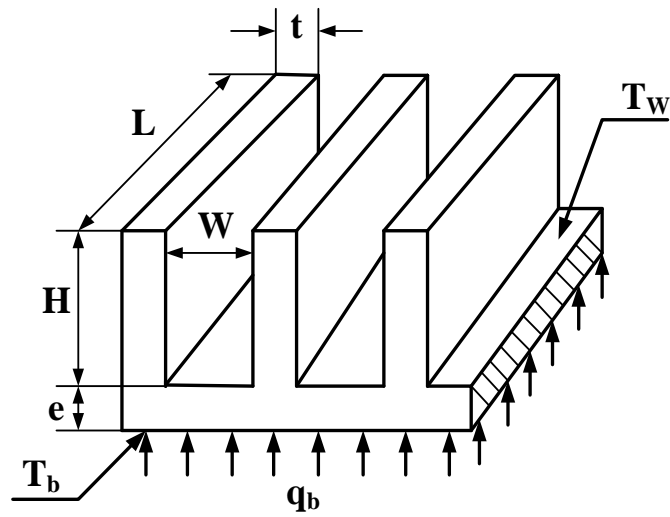
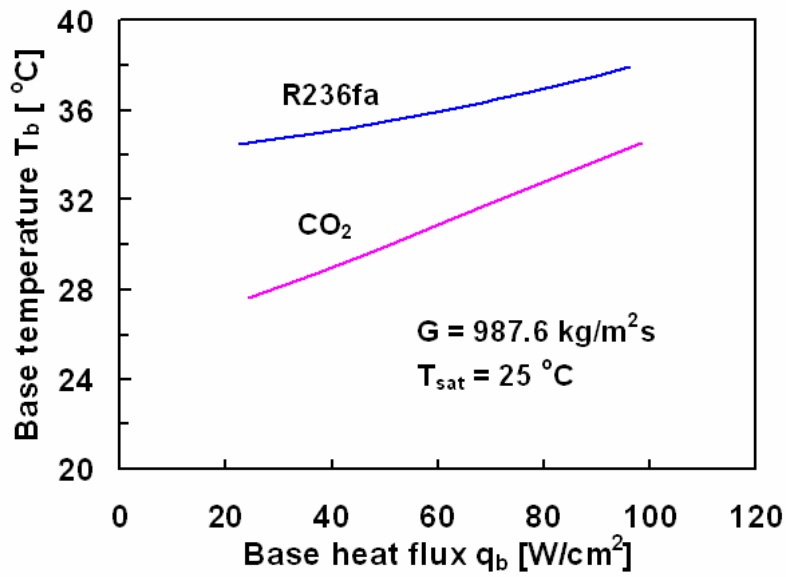


Figure 2. Scanning electron microscope photograph of the multi-micro-channels at three different scales. The middle and bottom figures are close-ups of the fin wall by Agostini e al. [51].



(a)



(b)

Figure 3. (a) Schematic diagram of a silicon multi-microchannel evaporator used for chips cooling; (b) Comparisons of simulation results of base temperature of CO<sub>2</sub> and R236fa at the indicated conditions for chips cooling by Cheng and Thome [35].

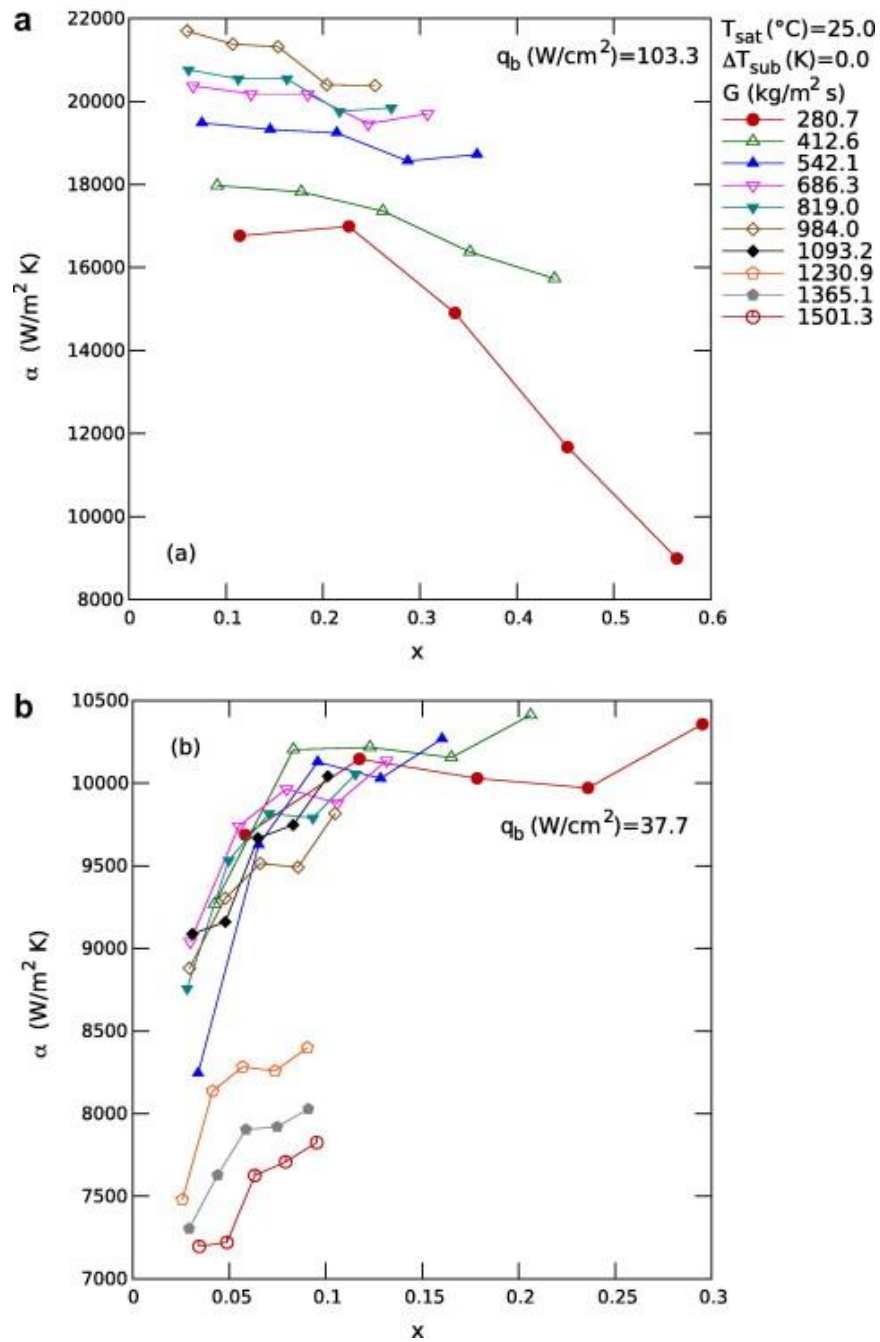


Figure 4. Measured local flow boiling heat transfer coefficient versus local vapour quality for various mass velocities, for the base heat fluxes of 37.7 (a) and 103.3 W/cm<sup>2</sup> (b) by Agostini et al. [52].

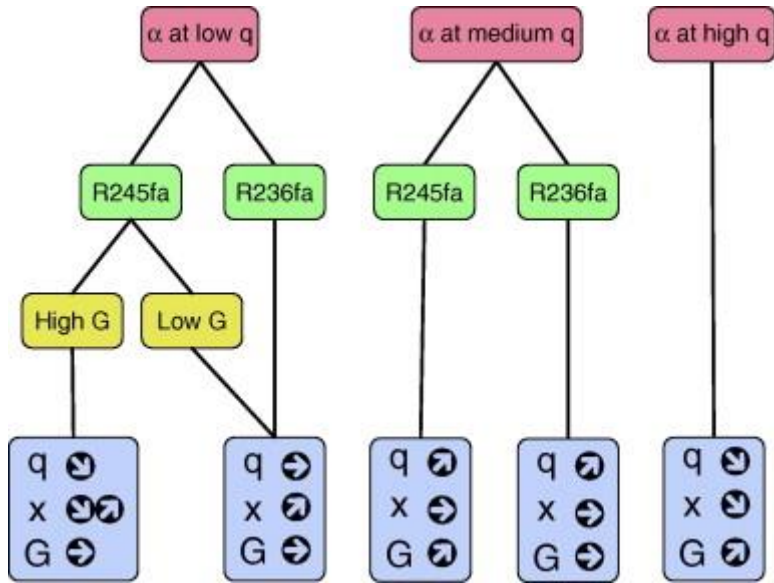


Figure 5. Heat transfer trends identified in the study for R245fa and R236fa: the arrows show the effect of the parameters heat flux  $q$ , vapor quality  $x$  and mass flux  $G$  on heat transfer coefficient  $\alpha$ , either increasing ( $\nearrow$ ), decreasing ( $\searrow$ ) or no effect ( $\rightarrow$ ) on  $\alpha$  by Agostini et al. [52].

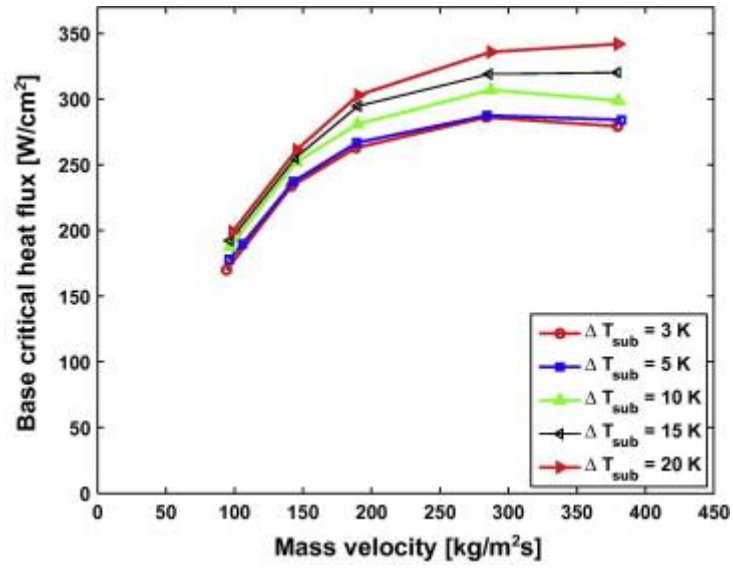


Figure 6. Experimental base CHF results for R134a at  $T_{sat} = 25^\circ\text{C}$  in the microchannel evaporator with deep  $H = 4052 \mu\text{m}$  channels by Park and Thome [54].

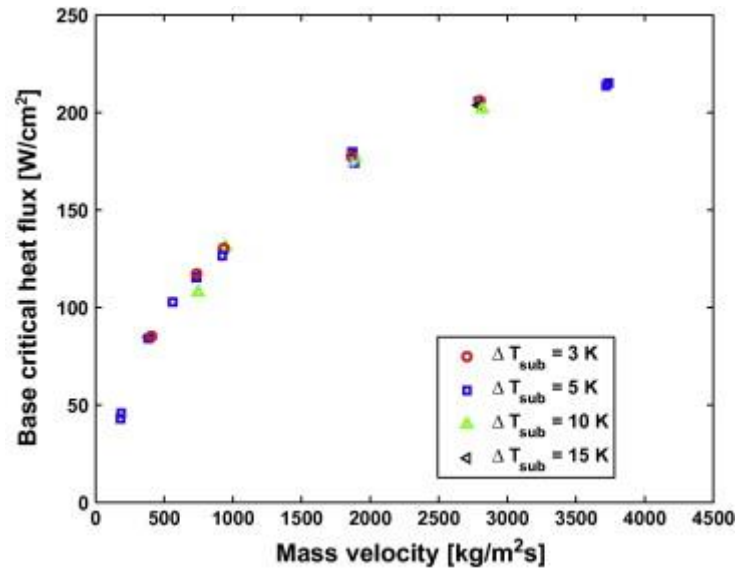


Figure 7. Experimental base CHF results for R134a at  $T_{sat} = 25^{\circ}\text{C}$  in the microchannel evaporator with deep  $H = 756 \mu\text{m}$  channels by Park and Thome [54].

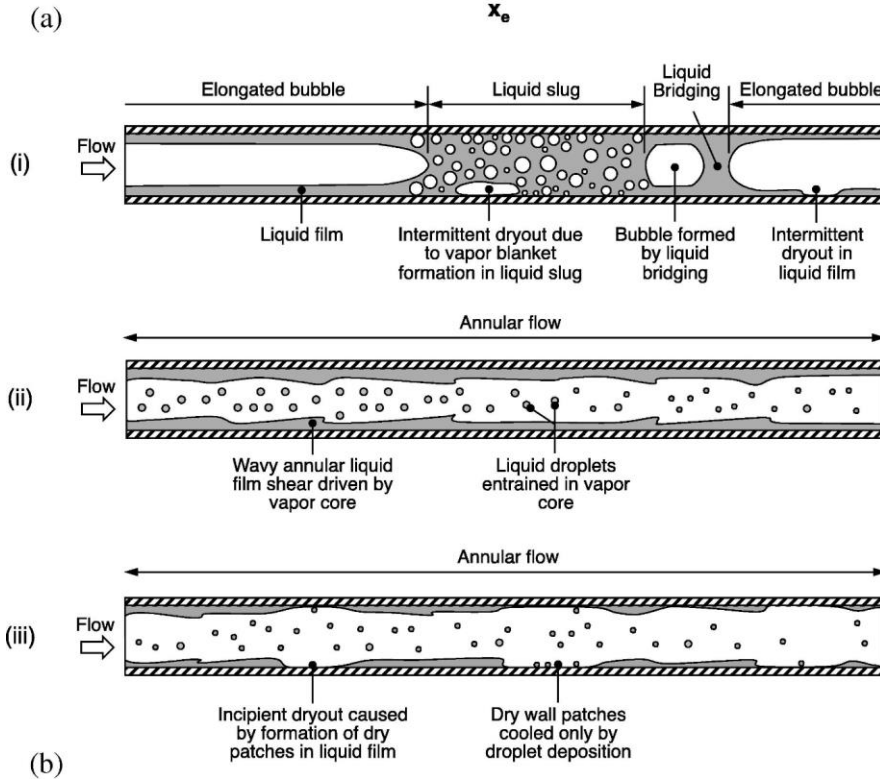
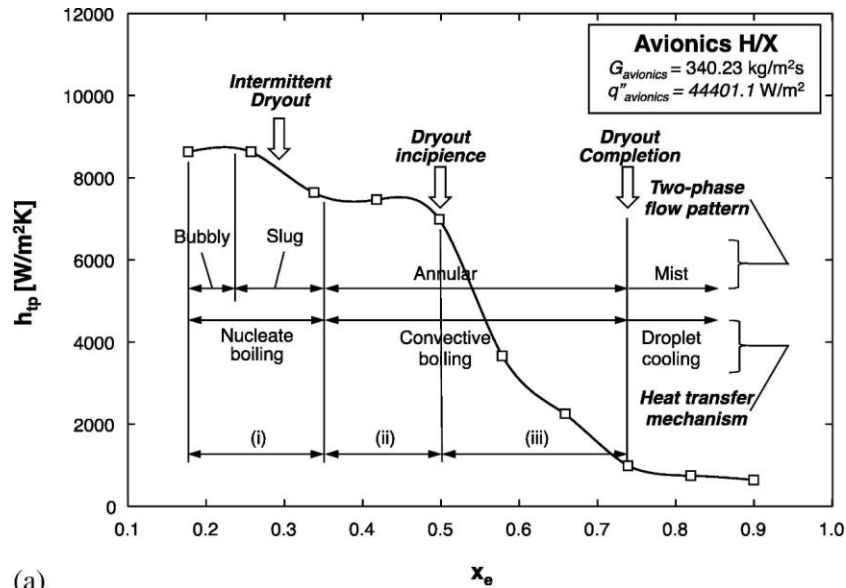


Figure 8. (a) Variation of heat transfer coefficient with axial distance in avionics heat exchanger (H/X) at  $G_{avionics} = 340.23 \text{ kg/m}^2\text{s}$  and  $q_{avionics} = 44,401.1 \text{ W/m}^2$ . (b) Schematics of flow boiling for the quality ranges in (a) illustrating dominant flow patterns and heat transfer mechanisms by Lee and Mudawar [50].

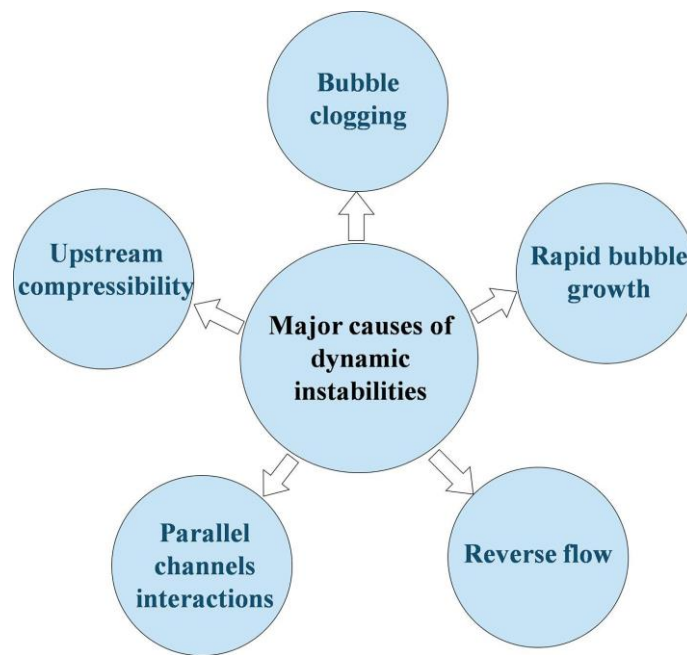


Figure 9. Major causes of flow boiling instabilities in microchannels by Prajapati and Bhandari [47].

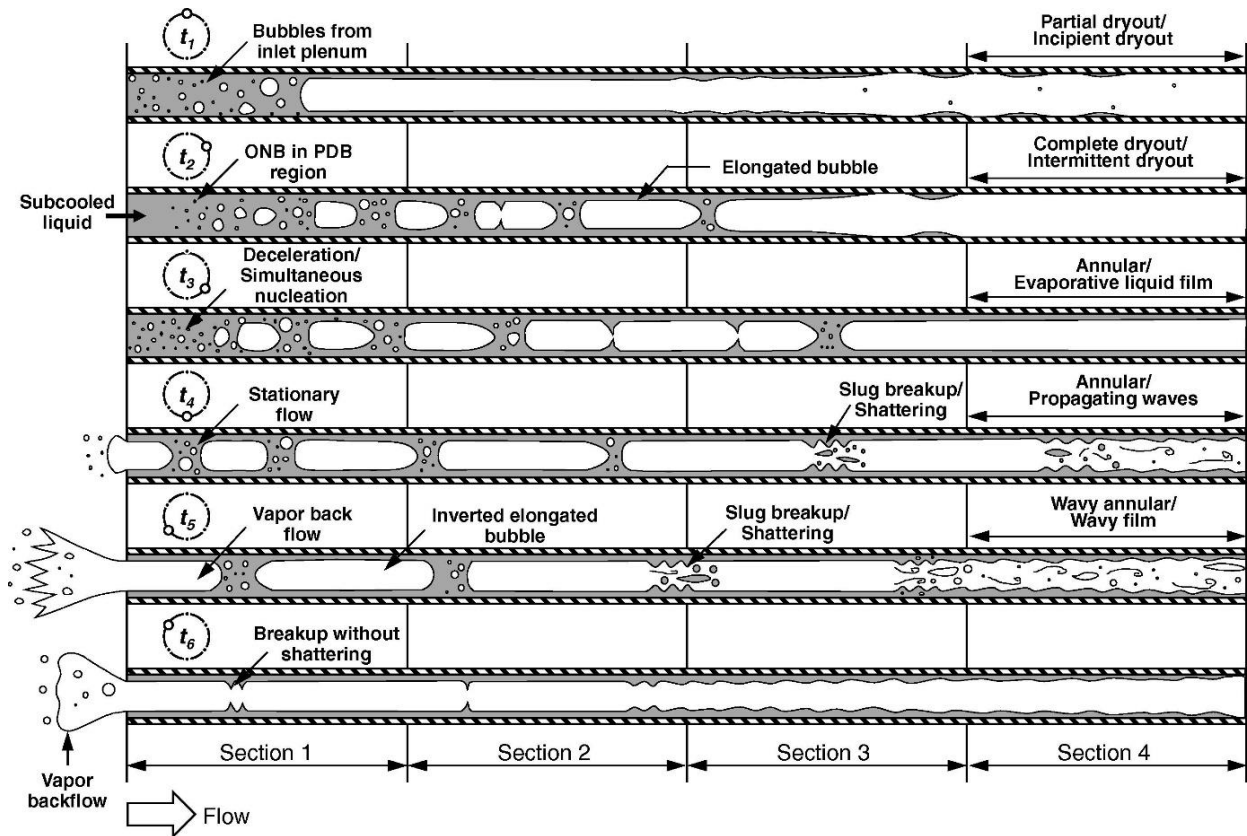


Figure 10. Schematic renderings of transient flow patterns observed at six different times within a single periodic cycle:  $t_1$ : beginning of the cycle,  $t_2$ : forward liquid advance,  $t_3$ : rapid bubble growth,  $t_4$ : commencement of transition pattern,  $t_5$ : commencement of wavy annular pattern, and  $t_6$ : end of liquid deficient period. The indicated sections are as follows: 1: subcooled boiling dominant, 2: combined saturated nucleate and convective boiling, 3: saturated convective boiling by annular film evaporation, and 4: intermittent dryout dominant region by Lee et al. [57].

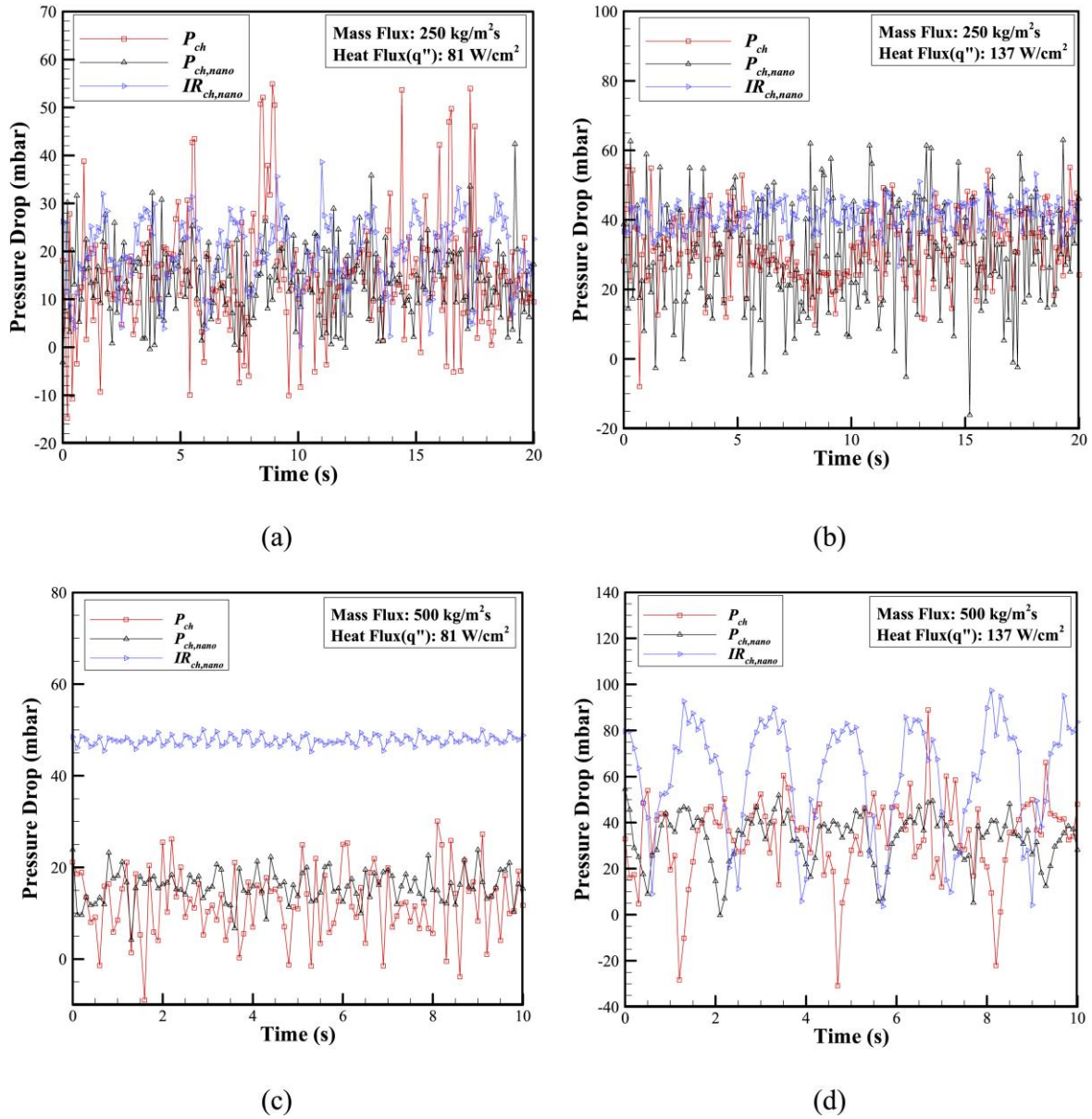
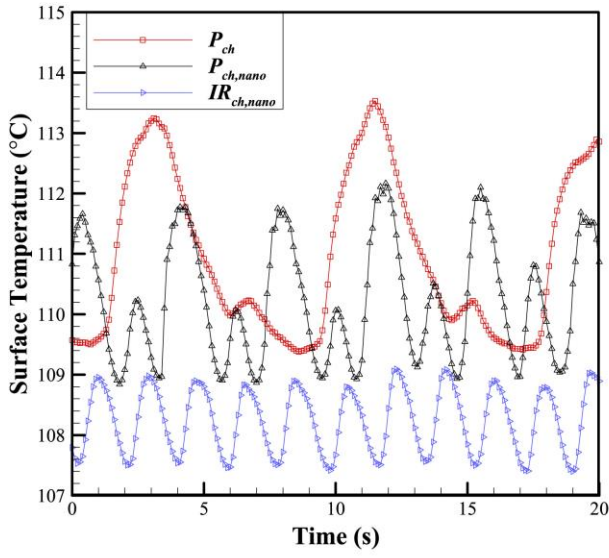
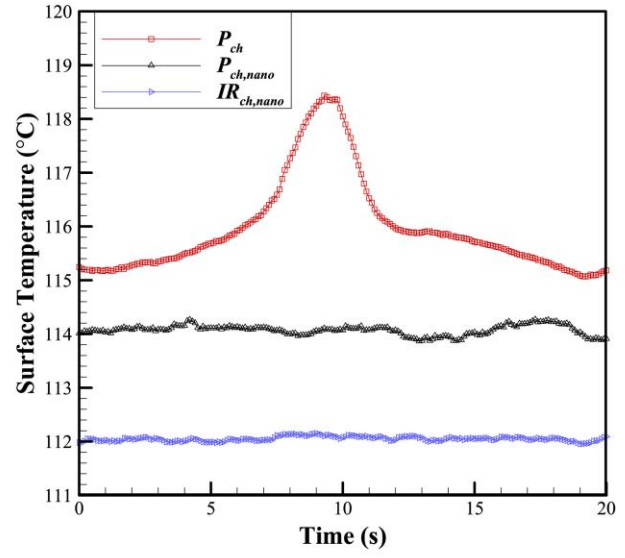


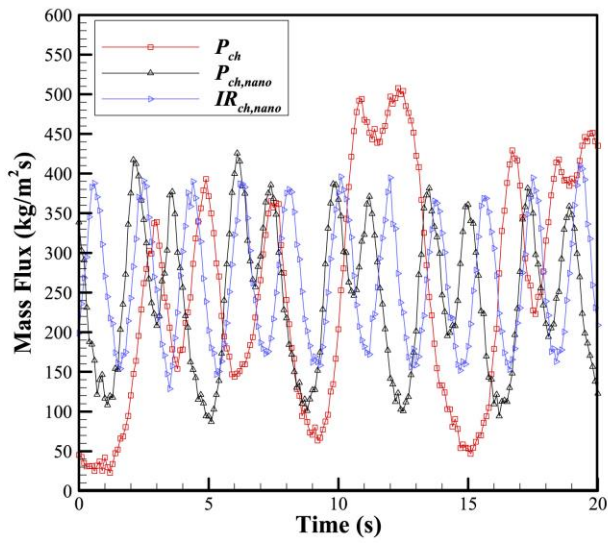
Figure 11. Temporal variation of pressure drop at (a) heat flux of  $81 \text{ W/cm}^2$  and mass velocity of  $250 \text{ kg/m}^2\text{s}$  and (b) heat flux of  $137 \text{ W/cm}^2$  and mass velocity of  $250 \text{ kg/m}^2\text{s}$ , (c) heat flux of  $81 \text{ W/cm}^2$  and mass velocity of  $500 \text{ kg/m}^2\text{s}$  and (d) heat flux of  $137 \text{ W/cm}^2$  and mass velocity of  $500 \text{ kg/m}^2\text{s}$  by Hedau et al. [65].



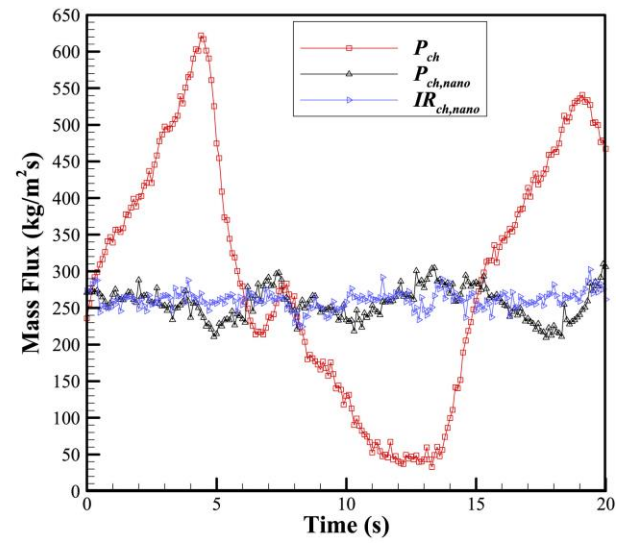
(a)



(b)



(c)



(d)

Figure 12. Fluctuations of the surface temperature at (a) heat flux of  $81 \text{ W/cm}^2$  and (b) heat flux  $137 \text{ W/cm}^2$  and fluctuations of mass velocity at (c) heat flux of  $81 \text{ W/cm}^2$  and (d) heat flux of  $137 \text{ W/cm}^2$  for mass velocity of  $250 \text{ kg/m}^2\text{s}$  by Hedau et al. [65].

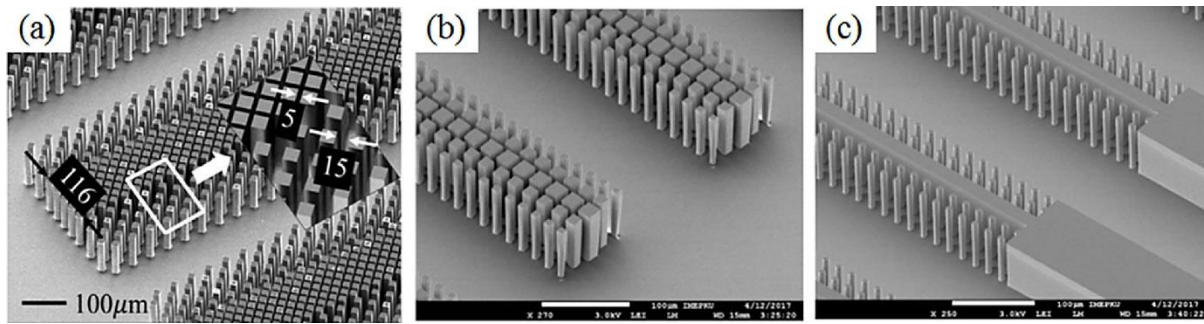


Figure 13. SEM images of (a) gradient-porous-wall microchannel [78]; (b) microchannels with gradient micro pin fins [81]; (c) rectangular porous-wall microchannel with uniform circular pin fins [79] by Deng et al. [75].

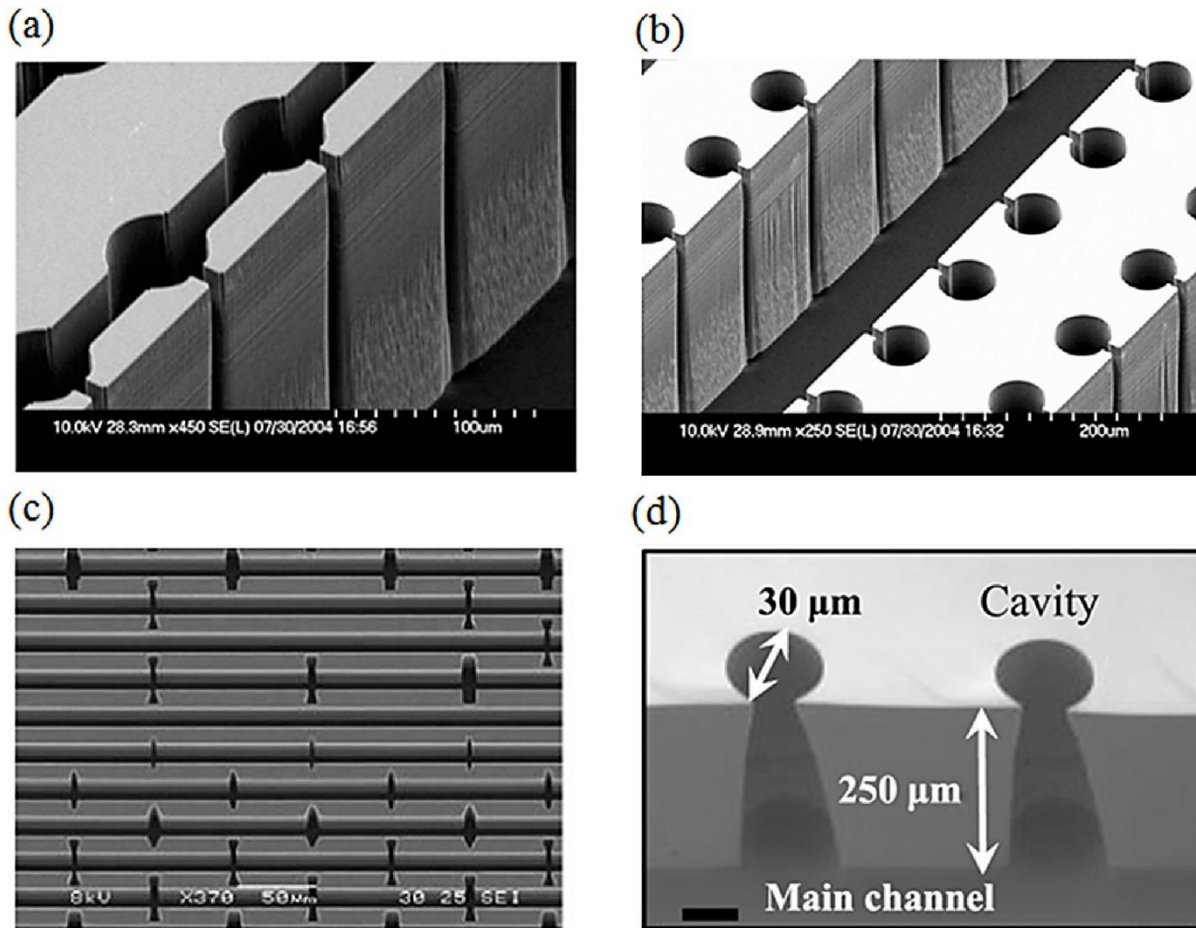


Figure 14. Microscopic images of microchannels with (a) interconnected reentrant cavities [90], (b) nonconnected reentrant cavity [91], (c) different shaped reentrant cavities [92], (d) reentrant microcavities on the sidewall [93] by Deng et al. [75].

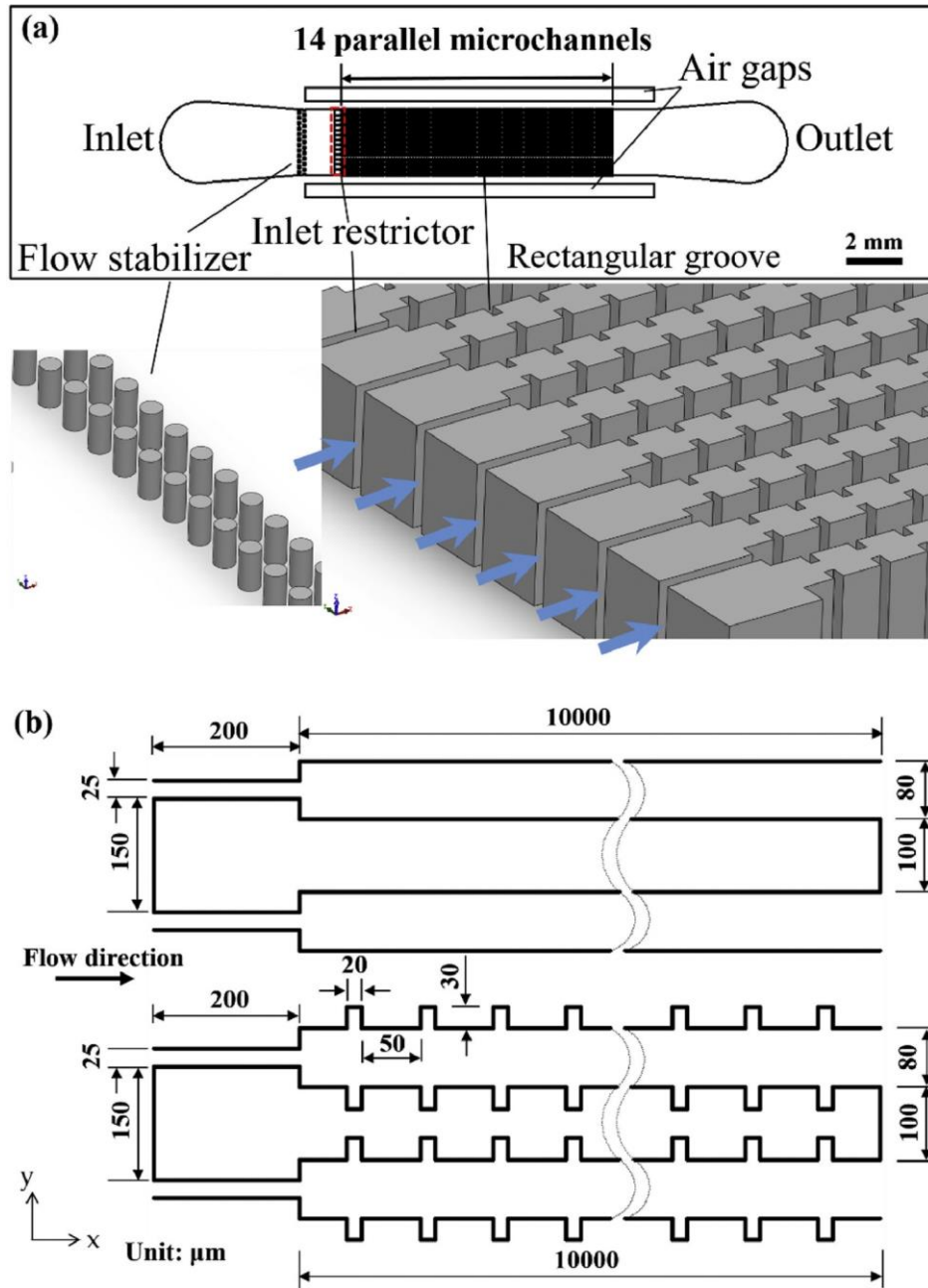


Figure 15. (a) Design of the microchannel heat sink; (b) Detailed parameters of the two microchannels by Cheng and Wu [82].

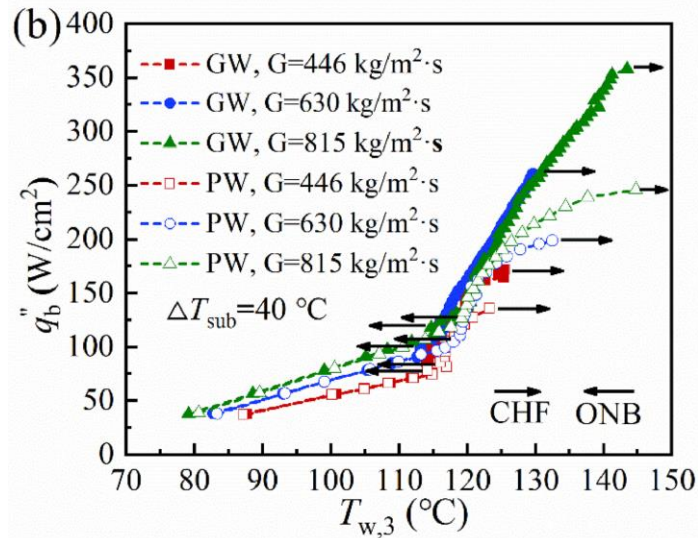
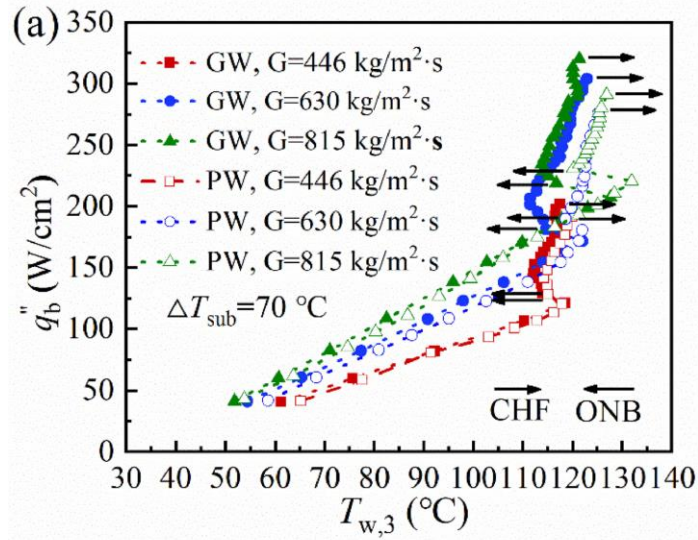


Figure 16. Typical V-shaped heat transfer coefficient curves for the microchannels with plain wall (PW) and groove wall (GW). The effective heat transfer coefficients are depicted versus (a) the effective heat flux and (b) the exit vapor quality (working fluid of DI-water) by Cheng and Wu [82].

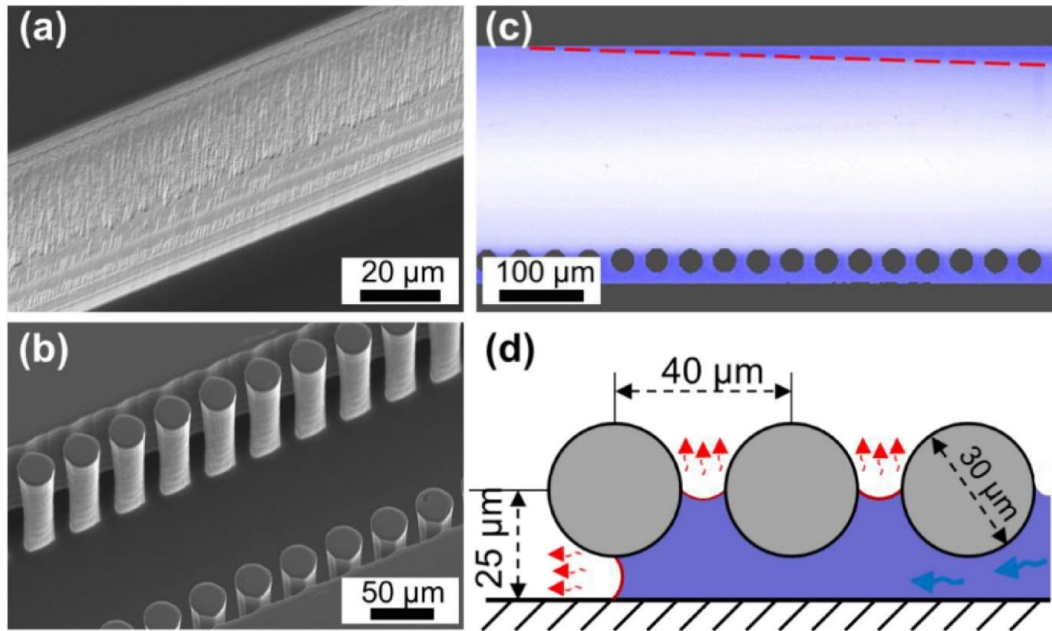


Figure 17. Development of conceptualization. (a) The SEM image of plain wall, (b) a SEM image of micro-pinfin fences, (c) the top-view of the receding liquid profile on the smooth wall and the one on the wall with micro-pinfin fences (re-colored image, blue represents liquid of water) and, (d) schematic of the thin film evaporation within micro-pinfin fence by Li et al. [86].

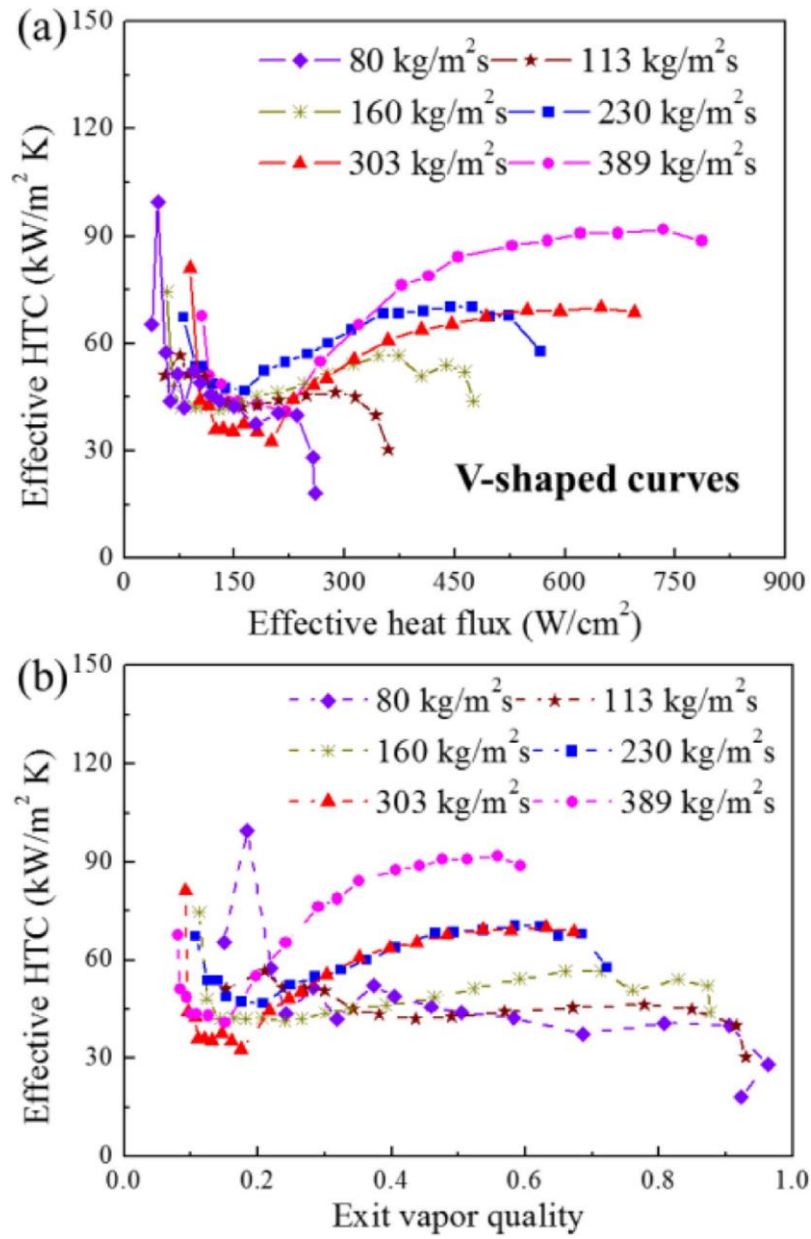


Figure 18. Boiling curves plotted with base heat flux (a)  $\Delta T_{\text{sub}}=70\text{ }^{\circ}\text{C}$  and (b)  $\Delta T_{\text{sub}}=40\text{ }^{\circ}\text{C}$  by Li et al. [86].

## Notes on contributors



Lixin Cheng has worked at Sheffield Hallam University since 2016. He obtained his Ph.D. in Thermal Energy Engineering at the State Key Laboratory of Multiphase Flow at Xi'an Jiaotong University, China in 1998. He has received several prestigious awards such as Alexander von Humboldt Fellowship in Germany in 2006, an ERCOFTAC Visitor Grant in Switzerland in 2010 and a Distinguished Visiting Professorship of the City of Beijing, China in 2015. His research interests are multiphase flow and heat transfer and thermal energy engineering. He has published more than 100 papers in journals and conferences, 9 book chapters and edited 10 books. He has delivered more than 60 keynote and invited lectures worldwide. He has been the chair of the *World Congress on Momentum, Heat and Mass Transfer (MHMT)* since 2017. He is one of the founders and co-chair of the *International Symposium of Thermal-Fluid Dynamics (ISTFD)* series since 2019. He is associate editor of *Heat Transfer Engineering*, *Heat Transfer Research* and *Journal of Fluid Flow, Heat and Mass Transfer*, and international advisor of *Thermal Power Generation* (a Chinese journal).



Guodong Xia is a leading professor in Thermal Energy Engineering at Beijing University of Technology, China. He received his Ph.D. in Thermal Energy Engineering at the State Key Laboratory of Multiphase Flow of Xi'an Jiaotong University, China in 1996. He was a visiting professor in the Institute of Process Engineering at the University of Hanover, Germany in 2000 -2001. His research interests include fundamentals and applications of microscale heat transfer, multiphase flow and heat transfer, waste energy recovery, thermal energy system, heat

exchanger design and enhanced heat transfer. He is a member of the multiphase flow committee of the Chinese Society of Engineering Thermophysics and a member of the multiphase flow committee of the Chinese Society of Theoretical and Applied Mechanics. He has published more than 150 papers in journals and conferences.